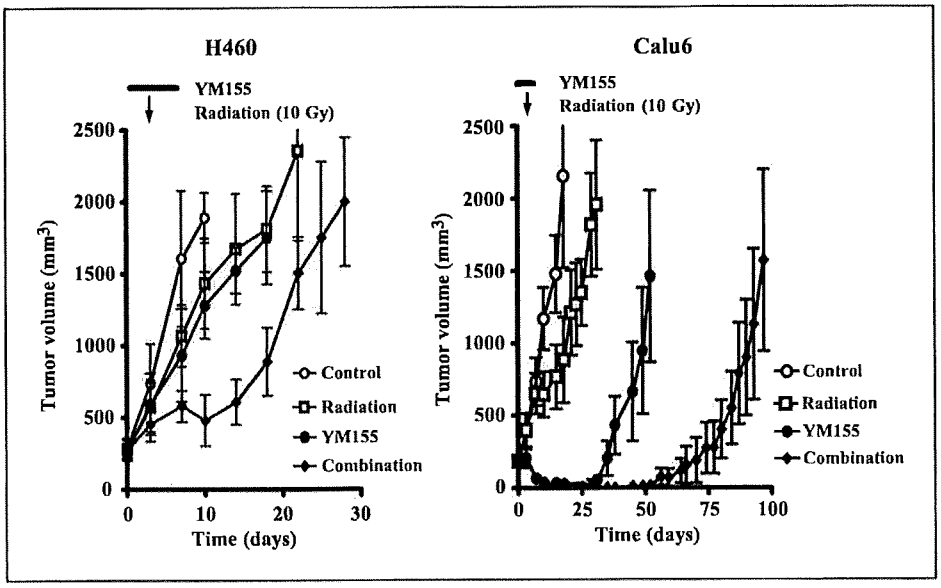

Fig. 5. Effect of YM155 on the growth of H460 or Calu6 tumors in mice subjected to single-dose radiotherapy. Cells were injected into the right hind limb of nude mice and allowed to grow. The mice were divided into four treatment groups: control, radiation alone, YM155 alone, or the combination of YM155 and radiation. YM155 (5 mg/kg) or vehicle was administered by continuous infusion over 7 d, and mice in the radiation groups were subjected to γ-irradiation with a single dose of 10 Gy on day 3 of drug treatment. Tumor volume was measured at the indicated times after the onset of treatment. Points, means from eight mice per group; bars, SE.

did not induce polyploidy (data not shown), suggesting that YM155-induced radiosensitization in the present study was not attributable to cell division defects caused by survivin depletion. Survivin was previously suggested to enhance tumor cell survival after radiation exposure through regulation of DSB repair (21). We therefore investigated the effect of YM155 on the repair of radiation-induced DSBs by immunofluorescence imaging of γ-H2AX foci. H2AX is a histone that is phosphorylated by ataxia telangiectasia mutated and DNA-dependent protein kinase in response to the generation of DSBs (45, 46). This reaction occurs rapidly, with half-maximal amounts of γ-H2AX generated within 1 minute and maximal amounts within 10 minutes (47), and a linear relation has been shown between the number of γ-H2AX foci and that of DSBs (48). The number of γ-H2AX foci is thus a sensitive and specific indicator of the existence of DSBs, with a decrease in this number reflecting DSB repair. We found that YM155 inhibited the repair of radiation-induced DSBs in NSCLC cells. If left unrepaired, DSBs can result in chromosome loss or cell death; agents that inhibit such repair thus increase the sensitivity of cells to ionizing radiation (49, 50). Our results therefore suggest that inhibition of DSB repair by YM155 contributes to the radiosensitization induced by this drug. Given that suppression of survivin expression impairs the repair of radiation-induced DNA damage (9, 21), our results further suggest that inhibition of DNA repair by YM155 is attributable to down-regulation of survivin expression.

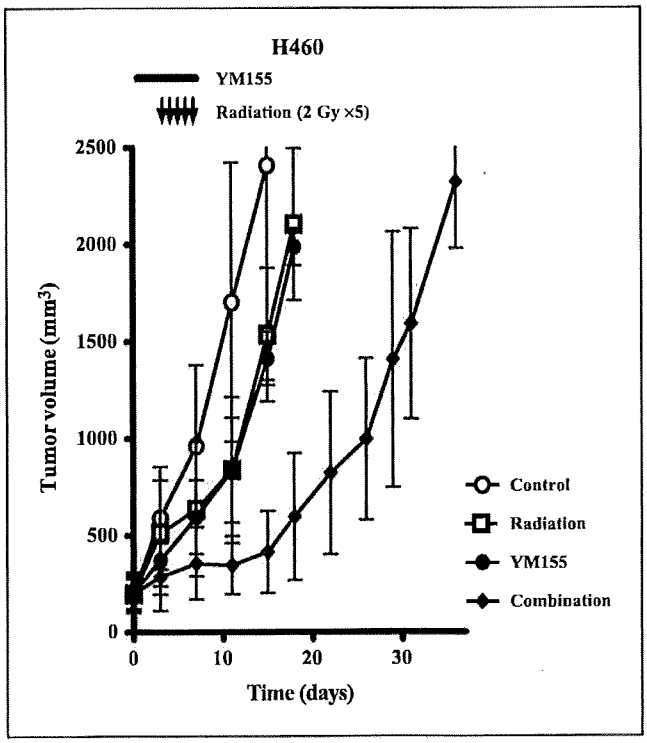

Fig. 6. Effect of YM155 on the growth of H460 tumors in mice subjected to fractionated radiotherapy. H460 cells were injected into the right hind limb of nude mice and allowed to grow. The mice were divided into four treatment groups: control, radiation alone, YM155 alone, or the combination of YM155 and radiation. YM155 (5 mg/kg) or vehicle was administered by continuous infusion over 7 d, and mice in the radiation groups were subjected to γ-irradiation with a daily dose of 2 Gy on days 3 to 7 of drug treatment. Tumor volume was measured at the indicated times after the onset of treatment. Points represent means from eight mice per group; bars represent SE.

The antitumor activity of YM155 has previously been shown to be time-dependent, with continuous infusion of the drug resulting in greater antitumor activity and less systemic toxicity compared with bolus injection in tumor xenograft models *in vivo* (14). Ongoing clinical trials of YM155 are thus being done with the drug administered on a continuous schedule. We also administered YM155 by continuous infusion in our *in vivo* experiments. The combination of YM155 with single-dose radiotherapy resulted in a marked increase in tumor growth delay compared with that apparent with either radiation or YM155 alone, indicating that YM155 enhanced the antitumor effect of ionizing radiation *in vivo*. Given that standard radiation therapy in the clinic is delivered according to a fractionated schedule, we also examined whether YM155 enhanced the tumor response to clinically relevant fractionated doses (2 Gy) of radiation. Indeed, YM155 was also effective in

enhancing the tumor response to such fractionated radiation. The enhancement factor with fractionated radiation (3.0) was similar to that observed with single-dose radiation (3.3) for H460 tumor xenografts.

Resistance to cytotoxic drugs and radiation is a major limiting factor in the treatment of cancer patients. Cross-resistance has been noted between radiotherapy and chemotherapy and has been attributed to defects in apoptosis signaling or to an enhanced capacity for DNA repair (51, 52). Our findings provide evidence that YM155 may break radioresistance by promoting apoptosis and inhibiting DNA repair. Previous studies have shown that suppression of survivin expression increases the sensitivity of tumor cells to chemotherapy(18, 53). It will therefore be of interest to determine whether YM155 also sensitizes tumor cells to chemotherapy.

In conclusion, we have shown that YM155 sensitizes NSCLC cells to radiation both *in vitro* and in animal models *in vivo*. The radiosensitization induced by YM155 seems to be attributable to the promotion of caspase-mediated apoptosis and inhibition of the repair of radiation-induced DNA damage. Our preclinical results provide a rationale for future clinical investigation of the therapeutic efficacy of YM155 in combination with radiotherapy.

Disclosure of Potential Conflicts of Interest

No potential conflicts of interest were disclosed.

Acknowledgments

We thank S. Ono for technical assistance.

References

1. Altieri DC. Survivin and apoptosis control. Adv Cancer Res 2003;88:31–52.
2. Altieri DC. Validating survivin as a cancer therapeutic target. Nat Rev Cancer 2003;3:46–54.
3. Wheatley SP, Carvalho A, Vagnarelli P, Earnshaw WC. INCENP is required for proper targeting of Survivin to the centromeres and the anaphase spindle during mitosis. Curr Biol 2001;11:886–90.
4. Ambrosini G, Adida C, Altieri DC. A novel anti-apoptosis gene, survivin, expressed in cancer and lymphoma. Nat Med 1997;3:917–21.
5. Marusawa H, Matsuzawa S, Welsh K, et al. HBXIP functions as a cofactor of survivin in apoptosis suppression. EMBO J 2003;22:2729–40.
6. Altieri DC. Molecular circuits of apoptosis regulation and cell division control: the survivin paradigm. J Cell Biochem 2004;92:656–63.
7. Monzo M, Rosell R, Felip E, et al. A novel anti-apoptosis gene: Re-expression of survivin messenger RNA as a prognosis marker in non-small-cell lung cancers. J Clin Oncol 1999;17:2100–4.
8. Altieri DC. The molecular basis and potential role of survivin in cancer diagnosis and therapy. Trends Mol Med 2001;7:542–7.
9. Rodel F, Hoffmann J, Distel L, et al. Survivin as a radioresistance factor, and prognostic and therapeutic target for radiotherapy in rectal cancer. Cancer Res 2005;65:4881–7.
10. Adida C, Berrebi D, Peuchmaur M, Reyes-Mugica M, Altieri DC. Anti-apoptosis gene, survivin, and prognosis of neuroblastoma. Lancet 1998;351:882–3.
11. Li F, Ackermann EJ, Bennett CF, et al. Pleiotropic cell-division defects and apoptosis induced by interference with survivin function. Nat Cell Biol 1999;1:461–6.
12. Olie RA, Simoes-Wust AP, Baumann B, et al. A novel antisense oligonucleotide targeting survivin expression induces apoptosis and sensitizes lung cancer cells to chemotherapy. Cancer Res 2000;60:2805–9.
13. Grossman D, Kim PJ, Schechner JS, Altieri DC. Inhibition of melanoma tumor growth *in vivo* by survivin targeting. Proc Natl Acad Sci U S A 2001;98:635–40.
14. Nakahara T, Takeuchi M, Kinoyama I, et al. YM155, a Novel Small-Molecule Survivin Suppressant, Induces Regression of Established Human Hormone-Refractory Prostate Tumor Xenografts. Cancer Res 2007;67:8014–21.
15. Milella M, Kornblau SM, Estrov Z, et al. Therapeutic targeting of the MEK/MAPK signal transduction module in acute myeloid leukemia. J Clin Invest 2001;108:851–9.
16. Carter BZ, Milella M, Altieri DC, Andreeff M. Cytokine-regulated expression of survivin in myeloid leukemia. Blood 2001;97:2784–90.
17. O'Connor DS, Wall NR, Porter AC, Altieri DC. A p34(cdc2) survival checkpoint in cancer. Cancer Cell 2002;2:43–54.
18. Wall NR, O'Connor DS, Plescia J, Pommier Y, Altieri DC. Suppression of survivin phosphorylation on Thr34 by flavopiridol enhances tumor cell apoptosis. Cancer Res 2003;63:230–5.
19. De Schepper S, Bruwiere H, Verhulst T, et al. Inhibition of histone deacetylases by chlamydocin induces apoptosis and proteasome-mediated degradation of survivin. J Pharmacol Exp Ther 2003;304:881–8.
20. Sah NK, Munshi A, Hobbs M, Carter BZ, Andreeff M, Meyn RE. Effect of downregulation of survivin expression on radiosensitivity of human epidermoid carcinoma cells. Int J Radiat Oncol Biol Phys 2006;66:852–9.
21. Chakravarti A, Zhai GG, Zhang M, et al. Survivin enhances radiation resistance in primary human glioblastoma cells via caspase-independent mechanisms. Oncogene 2004;23:7494–506.
22. Pennati M, Binda M, Colella G, et al. Radiosensitization of human melanoma cells by ribozyme-mediated inhibition of survivin expression. J Invest Dermatol 2003;120:648–54.
23. Cao C, Mu Y, Hallahan DE, Lu B. XIAP and survivin as therapeutic targets for radiation sensitization in preclinical models of lung cancer. Oncogene 2004;23:7047–52.
24. Lu B, Mu Y, Cao C, et al. Survivin as a therapeutic target for radiation sensitization in lung cancer. Cancer Res 2004;64:2840–5.
25. Kappler M, Taubert H, Bartel F, et al. Radiosensitization, after a combined treatment of survivin siRNA and irradiation, is correlated with the activation of caspases 3 and 7 in a wt-p53 sarcoma cell line, but not in a mt-p53 sarcoma cell line. Oncol Rep 2005;13:167–72.
26. Ikeda M, Okamoto I, Tamura K, et al. Down-regulation of survivin by ultraviolet C radiation is dependent on p53 and results in G(2)-M arrest in A549 cells. Cancer Lett 2007;248:292–8.
27. Albert JM, Cao C, Kim KW, et al. Inhibition of poly(ADP-ribose) polymerase enhances cell death and improves tumor growth delay in irradiated lung cancer models. Clin Cancer Res 2007;13:3033–42.
28. United Kingdom Co-ordinating Committee on Cancer Research (UKCCCR) Guidelines for the Welfare of Animals in Experimental Neoplasia (Second Edition). Br J Cancer 1998;77:1–10.
29. Johnson ME, Howerth EW. Survivin: a bifunctional inhibitor of apoptosis protein. Vet Pathol 2004;41:599–607.
30. Difilippantonio MJ, Zhu J, Chen HT, et al. DNA repair protein Ku80 suppresses chromosomal aberrations and malignant transformation. Nature 2000;404:510–4.
31. Gao Y, Ferguson DO, Xie W, et al. Interplay of p53 and DNA-repair protein XRCC4 in tumorigenesis, genomic stability and development. Nature 2000;404:897–900.
32. Facchetti F, Previdi S, Ballarini M, Minucci S, Perego P, La Porta CA. Modulation of pro- and anti-apoptotic factors in human melanoma cells exposed to histone deacetylase inhibitors. Apoptosis 2004;9:573–82.
33. Grimm D, Kay MA. RNAi and gene therapy: a mutual attraction. Hematology Am Soc Hematol Educ Program 2007;2007:473–81.
34. Nakagawa K, Satoh T, Okamoto I, et al. Phase I study of YM155, a new first-in-class survivin suppressant, in patient with advanced solid tumors in Japan [abstract 3536]. ASCO 2007;25:18S.
35. Fertil B, Malaise EP. Intrinsic radiosensitivity of human cell lines is correlated with radioresponsiveness of human tumors: analysis of 101 published survival curves. Int J Radiat Oncol Biol Phys 1985;11:1699–707.
36. Fulda S, Debatin KM. Targeting apoptosis pathways in cancer therapy. Curr Cancer Drug Targets 2004;4:569–76.
37. Olive PL, Durand RE. Apoptosis: an indicator of radiosensitivity *in vitro*? Int J Radiat Biol 1997;71:695–707.
38. Dubray B, Breton C, Delic J, et al. *In vitro* radiation-induced apoptosis and tumour response to radiotherapy: a prospective study in patients with non-Hodgkin lymphomas treated by low-dose irradiation. Int J Radiat Biol; 1997. p. 759–60.
39. Aldridge DR, Radford IR. Explaining differences in sensitivity to killing by ionizing radiation between human lymphoid cell lines. Cancer Res 1998;58:2817–24.
40. Sirzen F, Zhivotovsky B, Nilsson A, Bergh J, Lewensohn R. Higher spontaneous apoptotic index in small cell compared with non-small cell lung carcinoma cell lines; lack of correlation with Bcl-2/Bax. Lung Cancer 1998;22:1–13.
41. Lawrence TS, Davis MA, Hough A, Rehemtulla A. The role of apoptosis in 2',2'-difluoro-2'-deoxycytidine (gemcitabine)-mediated radiosensitization. Clin Cancer Res 2001;7:314–9.
42. Meister N, Shalaby T, von Bueren AO, et al. Interferon-γ mediated up-regulation of caspase-8 sensitizes medulloblastoma cells to radio- and chemotherapy. Eur J Cancer 2007;43:1833–41.
43. Terada Y, Tatsuka M, Suzuki F, et al. AIM-1: a

mammalian midbody-associated protein required for cytokinesis. EMBO J 1998;17:667–76.
44. Uren AG, Wong L, Pakusch M, et al. Survivin and the inner centromere protein INCENP show similar cell-cycle localization and gene knockout phenotype. Curr Biol 2000;10:1319–28.
45. Burma S, Chen BP, Murphy M, Kurimasa A, Chen DJ. ATM phosphorylates histone H2AX in response to DNA double-strand breaks. J Biol Chem 2001;276:42462–7.
46. Stiff T, O'Driscoll M, Rief N, Iwabuchi K, Lobrich M, Jeggo PA. ATM and DNA-PK function redundantly to phosphorylate H2AX after exposure to ionizing radiation. Cancer Res 2004;64:2390–6.
47. Rogakou EP, Pilch DR, Orr AH, Ivanova VS, Bonner WM. DNA double-stranded breaks induce histone H2AX phosphorylation on serine 139. J Biol Chem 1998;273:5858–68.
48. Leatherbarrow EL, Harper JV, Cucinotta FA, O'Neill P. Induction and quantification of γ-H2AX foci following low and high LET-irradiation. Int J Radiat Biol 2006;82:111–8.
49. Taneja N, Davis M, Choy JS, et al. Histone H2AX phosphorylation as a predictor of radiosensitivity and target for radiotherapy. J Biol Chem 2004;279:2273–80.
50. Banath JP, Macphail SH, Olive PL. Radiation sensitivity, H2AX phosphorylation, and kinetics of repair of DNA strand breaks in irradiated cervical cancer cell lines. Cancer Res 2004;64:7144–9.
51. Bergman PJ, Harris D. Radioresistance, chemoresistance, and apoptosis resistance. The past, present, and future. Vet Clin North Am Small Anim Pract 1997;27:47–57.
52. Friesen C, Lubatschofski A, Kotzerke J, Buchmann I, Reske SN, Debatin KM. Beta-irradiation used for systemic radioimmunotherapy induces apoptosis and activates apoptosis pathways in leukaemia cells. Eur J Nucl Med Mol Imaging 2003;30:1251–61.
53. Yonesaka K, Tamura K, Kurata T, et al. Small interfering RNA targeting survivin sensitizes lung cancer cell with mutant p53 to adriamycin. Int J Cancer 2006;118:812–20.

Oncogene (2007), 1–12

www.nature.com/onc

ORIGINAL ARTICLE

Aberrant expression of Fra-2 promotes CCR4 expression and cell proliferation in adult T-cell leukemia

T Nakayama[1], K Hieshima[1], T Arao[2], Z Jin[1], D Nagakubo[1], A-K Shirakawa[1], Y Yamada[3], M Fujii[4], N Oiso[5], A Kawada[5], K Nishio[2] and O Yoshie[1]

[1]Department of Microbiology, Kinki University School of Medicine, Osaka, Japan; [2]Department of Genome Science, Kinki University School of Medicine, Osaka, Japan; [3]Department of Laboratory Medicine, Nagasaki University Graduate School of Biomedical Sciences, Nagasaki, Japan; [4]Division of Virology, Niigata University Graduate School of Medical and Dental Sciences, Niigata, Japan and [5]Department of Dermatology, Kinki University School of Medicine, Osaka, Japan

Adult T-cell leukemia (ATL) is a mature CD4$^+$ T-cell malignancy etiologically associated with human T-cell leukemia virus type 1 (HTLV-1). Primary ATL cells frequently express CCR4 at high levels. Since HTLV-1 Tax does not induce CCR4 expression, transcription factor(s) constitutively active in ATL may be responsible for its strong expression. We identified an activator protein-1 (AP-1) site in the CCR4 promoter as the major positive regulatory element in ATL cells. Among the AP-1 family members, Fra-2, JunB and JunD are highly expressed in fresh primary ATL cells. Consistently, the Fra-2/JunB and Fra-2/JunD heterodimers strongly activated the CCR4 promoter in Jurkat cells. Furthermore, Fra-2 small interfering RNA (siRNA) or JunD siRNA, but not JunB siRNA, effectively reduced CCR4 expression and cell growth in ATL cells. Conversely, Fra-2 or JunD overexpression promoted cell growth in Jurkat cells. We identified 49 genes, including c-Myb, BCL-6 and MDM2, which were downregulated by Fra-2 siRNA in ATL cells. c-Myb, BCL-6 and MDM2 were also downregulated by JunD siRNA. As Fra-2, these proto-oncogenes were highly expressed in primary ATL cells but not in normal CD4$^+$ T cells. Collectively, aberrantly expressed Fra-2 in association with JunD may play a major role in CCR4 expression and oncogenesis in ATL.
Oncogene advance online publication, 10 December 2007; doi:10.1038/sj.onc.1210984

Keywords: adult T-cell leukemia; CCR4; Fra-2; JunD; c-Myb; MDM2; BCL-6

Correspondence: Professor O Yoshie, Department of Microbiology, Kinki University School of Medicine, 377-2, Ohono-Higashi, Osaka-Sayama, Osaka 589-8511, Japan.
E-mail: o.yoshie@med.kindai.ac.jp
Received 29 May 2007; revised 29 October 2007; accepted 6 November 2007

Introduction

Adult T-cell leukemia (ATL) is a highly aggressive malignancy of mature CD4$^+$CD25$^+$ T cells etiologically associated with human T-cell leukemia virus type 1 (HTLV-1; Yamamoto and Hinuma, 1985). HTLV-1 encodes a potent viral transactivator Tax that activates the HTLV-1 long terminal repeat (LTR) and also induces the expression of various cellular target genes, including those encoding cytokines, cytokine receptors, chemokines, cell adhesion molecules and nuclear transcriptional factors, collectively leading to the strong promotion of cell proliferation (Yoshida, 2001; Grassmann *et al.*, 2005). However, ATL develops after a long period of latency, usually several decades, during which oncogenic progression is considered to occur through the accumulation of multiple genetic and epigenetic changes (Matsuoka, 2003). Furthermore, circulating ATL cells usually do not express Tax and are considered to be independent of Tax (Matsuoka, 2003). Previously, Mori *et al.* have demonstrated the strong constitutive activation of nuclear factor kappa B (NF-κB) and activator protein-1 (AP-1) in primary ATL cells (Mori *et al.*, 1999, 2000). However, the molecular mechanisms of ATL oncogenesis still remain largely unknown.

CCR4 is a chemokine receptor known to be selectively expressed by Th2 cells, regulatory T cells (Treg) and skin-homing effector/memory T cells (Imai *et al.*, 1999; Iellem *et al.*, 2001; Yoshie *et al.*, 2001). Previously, we and others showed that ATL cells in the majority of cases are strongly positive for surface CCR4 (Yoshie *et al.*, 2002; Ishida *et al.*, 2003; Nagakubo *et al.*, 2007). Ishida *et al.* have also demonstrated a significant correlation of CCR4 expression with skin involvement and poor prognosis in ATL patients (Ishida *et al.*, 2003). Furthermore, several groups have reported that FOXP3, a forkhead/winged helix transcription factor and a specific marker of Treg (Hori *et al.*, 2003), is frequently expressed in ATL (Karube *et al.*, 2004; Matsubara *et al.*, 2005), supporting the notion that at least a fraction of ATL cases are derived from Treg.

It is also notable that primary ATL cells express CCR4 at levels much higher than normal resting CD4$^+$CD25$^+$ T cells (Nagakubo *et al.*, 2007). Given

that CCR4 is not inducible by Tax (Yoshie *et al.*, 2002), transcription factor(s) constitutively active in ATL cells may be responsible for CCR4 expression. Here, we demonstrate that Fra-2, one of the AP-1 family members (Shaulian and Karin, 2002; Eferl and Wagner, 2003), is aberrantly expressed in primary ATL cells. We further demonstrate that the Fra-2/JunD heterodimer plays a major role in both CCR4 expression and cell proliferation in ATL cells. Furthermore, we demonstrate that the proto-oncogenes c-Myb, BCL-6 and MDM2 (Oh and Reddy, 1999; Pasqualucci *et al.*, 2003; Vargas *et al.*, 2003) are the downstream target genes of the Fra-2/JunD heterodimer and are highly expressed in primary ATL cells. Thus, aberrantly expressed Fra-2 in association with JunD may be involved in ATL oncogenesis.

Results

Analysis of CCR4 promoter activity in ATL-derived cell lines

To examine the transcriptional regulation of CCR4 expression in ATL, we constructed a reporter plasmid carrying the CCR4 promoter region from −983 to +25 bp (the major transcriptional initiation site, +1) fused with the luciferase reporter gene. As shown in Figure 1a, pGL3-CCR4 (−983/+25) showed much stronger promoter activities in ATL cell lines (HUT102 and ST1) than in control human T-cell lines (MOLT-4 and Jurkat). We therefore generated a series of 5′-truncated promoter plasmids and examined their activity in ATL cell lines. As shown in Figure 1b, the promoter region from −151 to −96 bp was the major positive regulatory region in both cell lines. The TFSEARCH program (http://mbs.cbrc.jp/research/db/TFSEARCH.html) revealed various potential transcriptional elements in this region (Figure 1c). To identify the actual regulatory elements, we introduced a mutation in each potential element and examined the promoter activity in ATL cell lines. As shown in Figure 1d, a mutation at the AP-1 site or the GATA-3 site significantly reduced the promoter activity. Moreover, double mutations targeting both sites further reduced the promoter activity.

Constitutive expression of Fra-2, JunB and JunD in primary ATL cells

AP-1 is known to be involved in tumorigenesis (Shaulian and Karin, 2002; Eferl and Wagner, 2003), while GATA-3 regulates Th2-type gene expression (Rengarajan *et al.*, 2000). Therefore, we focused on AP-1 in the subsequent study. AP-1 constitutes a heterodimer of a member of the Fos family (c-Fos, FosB, Fra-1 and Fra-2) and a member of the Jun family (c-Jun, JunB and JunD) or a homodimer of the Jun family (Shaulian and Karin, 2002; Eferl and Wagner, 2003). Even though AP-1 was shown to be constitutively active in primary ATL cells (Mori *et al.*, 2000), it has not been clarified which members of AP-1 are actually

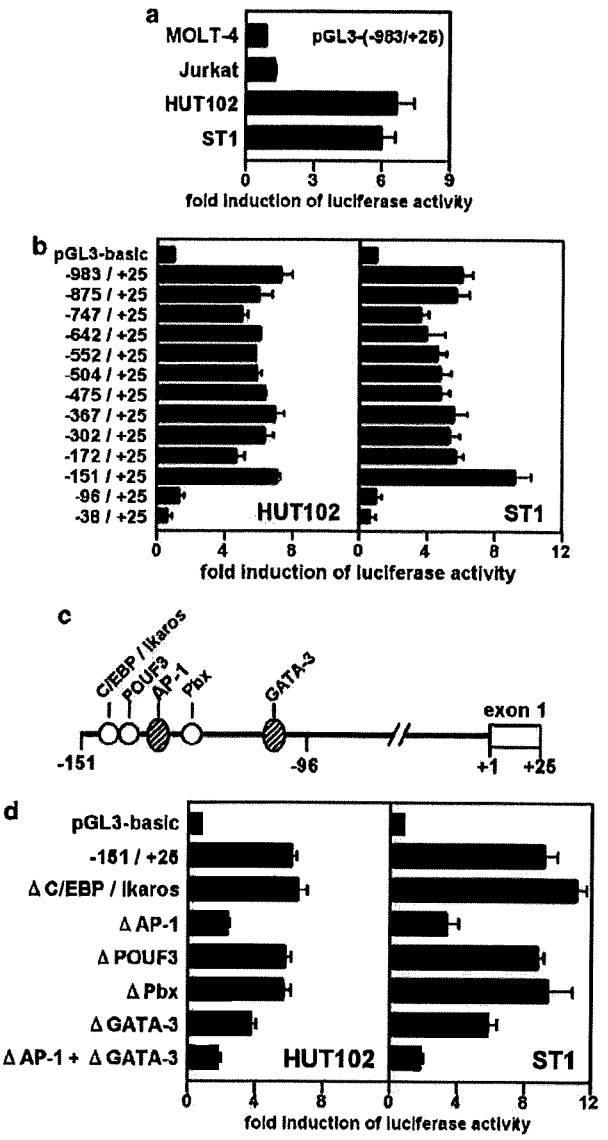

Figure 1 Identification of regulatory elements in the CCR4 promoter. Cells were transfected with pSV-β-galactosidase and pGL3-basic or pGL3-basic inserted with the CCR4 promoter regions as indicated. After 24–27 h, luciferase assays were performed. Promoter activation was expressed by the fold induction of luciferase activity in cells transfected with the CCR4 promoter–luciferase constructs versus cells transfected with the control pGL3-basic. Transfection efficiency was normalized by β-galactosidase activity. Each bar represents the mean ± s.e.m. from three separate experiments. (**a**) Selective activation of the CCR4 promoter in adult T-cell leukemia (ATL) cell lines. MOLT-4 and Jurkat: control human T-cell lines; HUT102 and ST1: ATL cell lines. (**b**) Deletion analysis. The promoter region from −151 to −96 bp is necessary and sufficient for reporter gene expression in the two ATL cell lines. (**c**) The schematic depiction of potential regulatory elements in the promoter region from −151 to −96 bp. (**d**) Mutation analysis. ΔC/EBP/Ikaros (from TCTTGGGAAA TGA to TCTTGCAAAATGA), ΔAP-1 (from AATGACTAAGA to AATGTCAAAGA), ΔPOUF3 (from CTTGGGAAATGA to CTTGGGAGGTGA), ΔPbx (from AAGAATCAT to AAGA CCCAT) and ΔGATA-3 (from TTCTATCAA to TTCTGACAA). The potential AP-1 and GATA-3 sites present within the −151 to −96 bp region are the major elements for CCR4 promoter activation in the two ATL cell lines.

expressed in primary ATL cells. We therefore first examined the mRNA expression of the AP-1 family members in primary ATL cells freshly isolated from patients in comparison with normal CD4+ T cells in resting, activated and Th1/Th2-polarized conditions (Figure 2a). As reported previously (Yoshie *et al.*, 2002; Nagakubo *et al.*, 2007), primary ATL cells consistently expressed CCR4 at levels much higher than various normal CD4+ T-cell populations, including Th2-polarized cultured T cells. Furthermore, primary ATL cells consistently expressed Fra-2 in sharp contrast to various normal CD4+ T-cell populations that were essentially negative for Fra-2 expression. Similar to various normal CD4+ T-cell populations, primary ATL

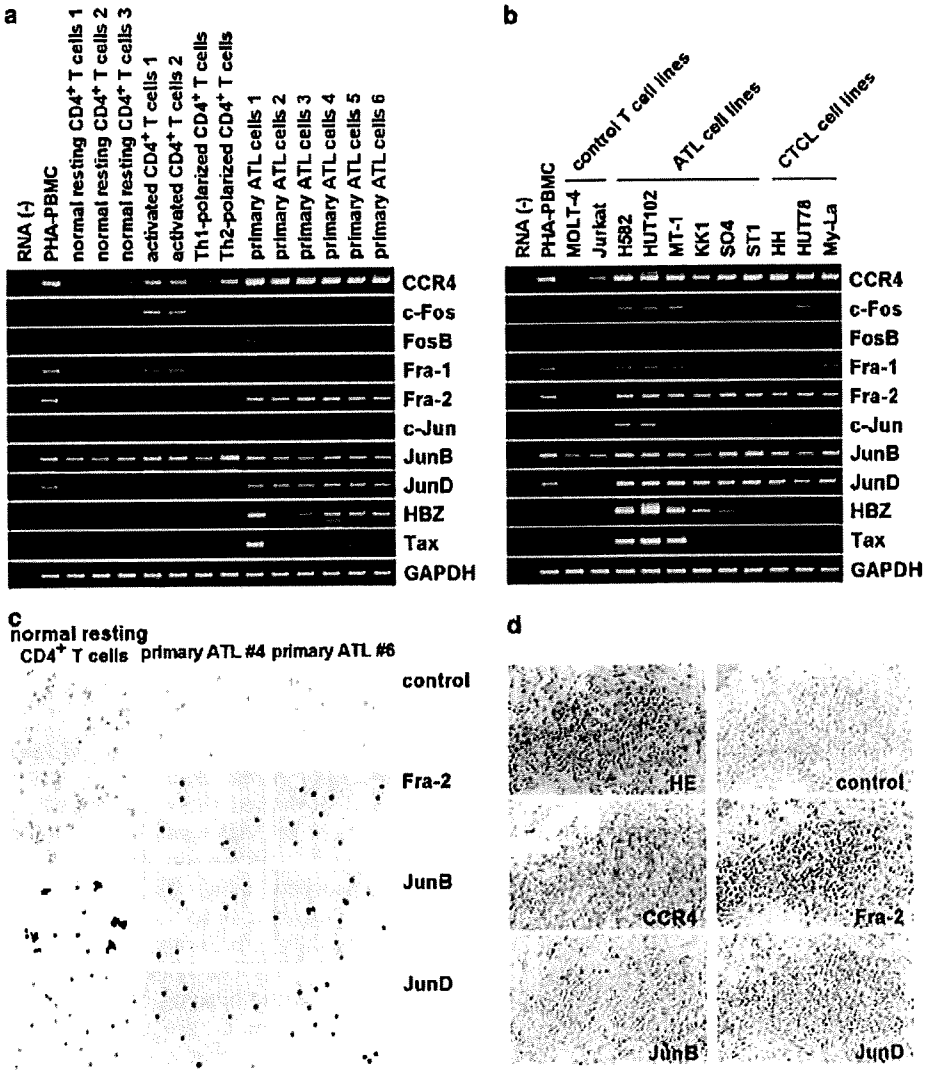

Figure 2 Constitutive expression of Fra-2, JunB and JunD in adult T-cell leukemia (ATL). (a) Reverse transcription (RT)–PCR analysis for the expression of the AP-1 family in normal T cells and primary ATL cells. Normal resting CD4+ T cells (purity, >96%) from healthy donors ($n=3$), activated CD4+ T cells from normal donors ($n=2$), Th1-polarized cultured CD4+ T cells, Th2-polarized cultured CD4+ T cells and freshly isolated primary ATL cells (>90% leukemic cells) from patients ($n=6$) were examined as indicated. Normal peripheral blood mononuclear cells treated with phytohemagglutinin (PHA-PBMC) served as a positive control. GAPDH served as a loading control. The representative results from at least two separate experiments are shown. (b) RT–PCR analysis for the expression of the AP-1 family in human T-cell lines. Two control human T-cell lines, six ATL cell lines and three CTCL cell lines were examined as indicated. PHA-PBMC served as a positive control. GAPDH served as a loading control. The representative results from two separate experiments are shown. (c) Immunocytochemical staining for Fra-2, JunB and JunD in normal CD4+ T cells and primary ATL cells. Normal CD4+ T cells from healthy donors (purity, >96%) and primary ATL cells (leukemic cells, >90%) from two patients were stained with anti-Fra-2, anti-JunB or anti-JunD. Normal rabbit IgG was used as the negative control (control). The representative results from two separate experiments are shown. Original magnification: ×400. (d) Immunohistochemical staining of CCR4, Fra-2, JunB and JunD in ATL skin lesions. Tissue sections from ATL skin lesions ($n=6$) were stained with anti-CCR4, anti-Fra-2, anti-JunB or anti-JunD. Mouse IgG_1 and normal rabbit IgG were used as the negative controls (control). Tissue sections were counterstained using Gill's hematoxylin. The representative results from a single donor are shown. Original magnification: ×400.

cells also constitutively expressed JunD and JunB even though JunD expression appeared to be upregulated in primary ATL cells. Other members of the AP-1 family were mostly negative in primary ATL cells, while activated normal CD4+ T cells expressed c-Fos, Fra-1 and c-Jun at high levels. There was no correlation in expression between Fra-2 and the virally encoded HTLV-1 basic leucine zipper factor HBZ or Tax in primary ATL cells. We also confirmed that Fra-2 is not inducible by Tax using JPX-9, a subline of Jurkat carrying the HTLV-1 Tax gene under the control of the metallothionein gene promoter (Nagata *et al.*, 1989; data not shown). Thus, the constitutive expression of Fra-2 is highly unique for primary ATL cells.

We also examined expression of the same set of genes in various human T-cell lines. As shown in Figure 2b, compared to control T-cell lines, ATL cell lines consistently expressed CCR4 and Fra-2 at high levels. ATL cell lines also expressed JunB and JunD at high levels. HTLV-1 Tax has been shown to induce various AP-1 family members (Nagata *et al.*, 1989; Iwai *et al.*, 2001), which may be involved in HTLV-1 gene expression and cell proliferation (Jeang *et al.*, 1991). Consistently, ATL cell lines expressing Tax (H582, HUT102 and MT-1) also expressed other AP-1 family members at low levels. Cutaneous T-cell lymphomas (CTCLs) are a subset of HTLV-1-negative T-cell lymphomas resembling ATL and known to be frequently positive for CCR4 (Kim *et al.*, 2005). CTCL cell lines were also found to strongly express CCR4, Fra-2, JunB and JunD. Thus, the constitutive expressions of Fra-2, JunB and JunD were shared by CCR4-expressing ATL and CTCL cell lines.

We also examined the Fra-2, JunB and JunD protein expression in freshly isolated primary ATL cells and normal resting CD4+ T cells. As shown in Figure 2c, primary ATL cells were indeed stained strongly positive for Fra-2, while normal CD4+ T cells were totally negative for Fra-2. Primary ATL cells were also strongly positive for JunB and JunD, while normal CD4+ T cells were variably positive for JunB and JunD at the single cell level. These results were highly consistent with the results from reverse transcription (RT)–PCR; Figure 2a). We also confirmed the CCR4, Fra-2, JunB and JunD protein expression in skin-infiltrating ATL cells (Figure 2d).

Activation of the CCR4 promoter by Fra-2/JunB and Fra-2/JunD heterodimers

AP-1 is known to function as a heterodimer of a member of the Fos family (c-Fos, FosB, Fra-1 and Fra-2) and a member of the Jun family (c-Jun, JunB and JunD) or a homodimer of the Jun family (Shaulian and Karin, 2002; Eferl and Wagner, 2003). We, therefore, next examined the activation of the CCR4 promoter by individual AP-1 family members singly or in combination. As recipients, we used two T-cell lines, namely, MOLT-4 and Jurkat. The expression levels of AP-1 members, including Fra-2, JunB and JunD, were very low in these cell lines (Figure 2b). As shown in Figure 3a, only Fra-2/JunB or Fra-2/JunD potently activated the CCR4 promoter in both cell lines. We confirmed that other members of the AP-1 family (c-Fos, FosB, Fra-1 and c-Jun) were transcriptionally active by using a synthetic promoter containing two tandem AP-1 consensus-binding sites (pGL3-2xAP-1; Figure 3b). Thus, among the AP-1 family members, only the Fra-2/JunB and Fra-2/JunD heterodimers are uniquely capable of activating the CCR4 promoter. This is highly consistent with their constitutive expression in primary ATL cells (Figure 2a).

Recently, the mRNA of HTLV-1 HBZ has been shown to be expressed in primary ATL cells (Satou *et al.*, 2006). We indeed observed the expression of HBZ in some primary ATL samples (Figure 2a). HBZ has been shown to activate JunB homodimer- or JunD homodimer-dependent transcription (Basbous *et al.*, 2003; Thebault *et al.*, 2004). Therefore, we also examined the effects of HBZ as well as Tax on the CCR4 promoter in MOLT-4 and Jurkat cells. As shown in Figure 3c, HBZ alone or in combination with Fra-2, JunB, JunD, Fra-2/JunB or Fra-2/JunD showed no effect on the activation of the CCR4 promoter. Similarly, Tax had no significant effect on the CCR4 promoter either alone or in combination with Fra-2, JunB, JunD, Fra-2/JunB or Fra-2/JunD. Thus, HTLV-1 encoded HBZ or Tax neither activates the CCR4 promoter nor affects its activation by Fra-2/JunB or Fra-2/JunD.

We have also confirmed that GATA-3 is constitutively expressed in primary ATL cells and activates the CCR4 promoter (data not shown). In normal CD4+ T cells, GATA-3 may be responsible for the selective expression of CCR4 in Th2 cells (Imai *et al.*, 1999; Rengarajan *et al.*, 2000).

Specific binding of Fra-2, JunB and JunD to the AP-1 site in the CCR4 promoter

We next examined the specific binding of AP-1 family members to the AP-1 site in the CCR4 promoter using the NoShift transcription factor assay, an enzyme-linked immunosorbent assay (ELISA)-like colorimetric assay that is an alternative to the electrophoretic mobility shift assay. As shown in Figure 4a, when the nuclear extracts of two control T-cell lines (MOLT-4 and Jurkat) were used, the specific binding of any AP-1 family members to the AP-1 site of the CCR4 promoter was hardly observed. On the other hand, when the nuclear extracts of two ATL cell lines (HUT102 and ST1) were used, we detected a high level of specific binding of Fra-2, JunB and JunD to the AP-1 site. These results are highly consistent with the results from RT–PCR analyses (Figure 2b) and the luciferase reporter assays (Figure 3a).

By using the chromatin immunoprecipitation (ChIP) assay, we further examined the binding of Fra-2, JunB and JunD to the AP-1 site of the CCR4 promoter *in vivo*. As shown in Figure 4b, we detected specific binding of Fra-2, JunB and JunD to the AP-1 site of the endogenous CCR4 promoter in primary ATL cells but not in normal CD4+ T cells. These results further

support the hypothesis that the CCR4 gene is a direct target gene of Fra-2/JunB and Fra-2/JunD heterodimers in primary ATL cells.

Effects of Fra-2, JunB and JunD small interfering RNAs on CCR4 expression and cell proliferation

To examine the role of Fra-2, JunB and JunD in CCR4 expression and cell proliferation in ATL cells, we next employed the small interfering RNA (siRNA) knockdown technique. As shown in Figure 5a, Fra-2 siRNA, JunB siRNA and JunD siRNA specifically reduced Fra-2 mRNA, JunB mRNA and JunD mRNA, respectively, in two ATL cell lines. On the other hand, control siRNA showed no such effect. Under these conditions, we examined the effects of these siRNAs on CCR4 expression and cell growth. As shown in Figure 5b, Fra-2 siRNA and JunD siRNA reduced CCR4 expression by approximately 50% in both cell lines, whereas JunB siRNA had hardly any inhibitory effect and control siRNA showed no inhibitory effect. Furthermore, as shown in Figure 5c, Fra-2 siRNA and JunD siRNA significantly reduced cell proliferation in both cell lines, whereas JunB siRNA or control siRNA did not. None of the siRNAs affected the growth of the control T-cell lines MOLT-4 and Jurkat. We also compared the effects of single and double knockdown of Fra-2 and JunD on cell growth in two ATL cell lines (Figure 5d). Compared to the effect of single knockdown of Fra-2 or JunD, no additive effect was observed by double knockdown of Fra-2 and JunD in both cell lines. These results may be consistent with the notion that Fra-2 and JunD promote growth in ATL cell lines by functioning as a heterodimer.

To further demonstrate the growth-promoting effects of Fra-2 and JunD, we performed stable transfection of Fra-2 and JunD in the control T-cell line Jurkat. As shown in Figure 5e, Jurkat cells overexpressing Fra-2 or JunD (see inset) indeed showed enhanced growth compared to those transfected with the vector alone. We were, however, unable to isolate Fra-2/JunD double transfectants in Jurkat, probably because of some adverse effects on Jurkat cells by the overexpression of both Fra-2 and JunD.

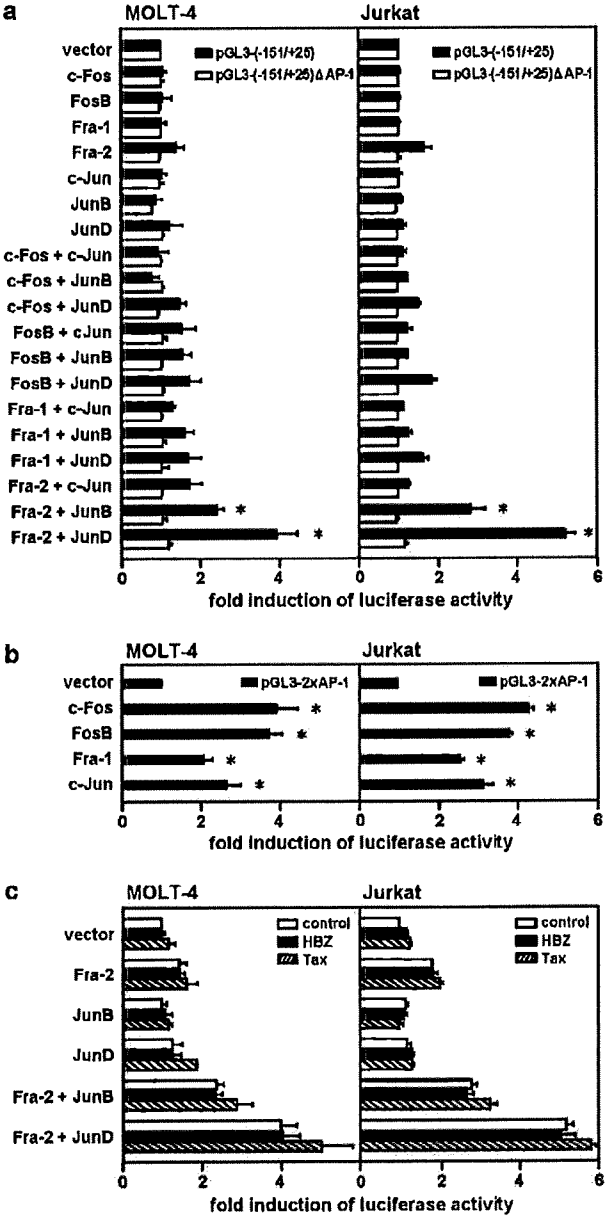

Figure 3 Transactivation of the CCR4 promoter by Fra-2/JunD and Fra-2/JunB. (a) Transactivation of the CCR4 promoter with or without the AP-1 site. MOLT-4 and Jurkat cells were cotransfected with pSV-β-galactosidase and pGL3-CCR4 (−151/+25) or pGL3-CCR4 (−151/+25)ΔAP-1 and an expression vector for c-Fos, FosB, Fra-1, Fra-2, c-Jun, JunB, JunD or a control vector as indicated. After 24–27 h, luciferase assays were performed in triplicate. Promoter activation was expressed as the fold induction of luciferase activity in cells transfected with an indicated AP-1 expression vector versus cells transfected with the vector alone. Transfection efficiency was normalized by β-galactosidase activity. Each bar represents the mean ± s.e.m. from three separate experiments. $^*P<0.05$. (b) Transactivation of a synthetic promoter with two copies of the consensus AP-1 site. MOLT-4 and Jurkat cells were cotransfected with pSV-β-galactosidase and pGL3-2xAP-1 and an expression vector for c-Fos, FosB, Fra-1, c-Jun or the vector alone as indicated. Promoter activation was expressed as the fold induction of luciferase activity in cells transfected with an indicated expression vector versus cells transfected with a control vector. After 24–27 h, luciferase assays were performed in triplicate. Transfection efficiency was normalized by β-galactosidase activity. Each bar represents the mean ± s.e.m. from three separate experiments. $^*P<0.05$. (c) Effect of HBZ or Tax on the activation of the CCR4 promoter. MOLT-4 and Jurkat cells were cotransfected with pSV-β-galactosidase and the pGL3-basic vector or pGL3-CCR4 (−151/+25) and an expression vector for Fra-2, JunB, JunD or a control vector and an expression vector for HBZ, Tax or a control vector as indicated. After 24–27 h, luciferase assays were performed in triplicate. Promoter activation was expressed as the fold induction of luciferase activity in cells transfected with an indicated expression vector versus cells transfected with a control vector. Transfection efficiency was normalized by β-galactosidase activity. Each bar represents the mean ± s.e.m. from three separate experiments.

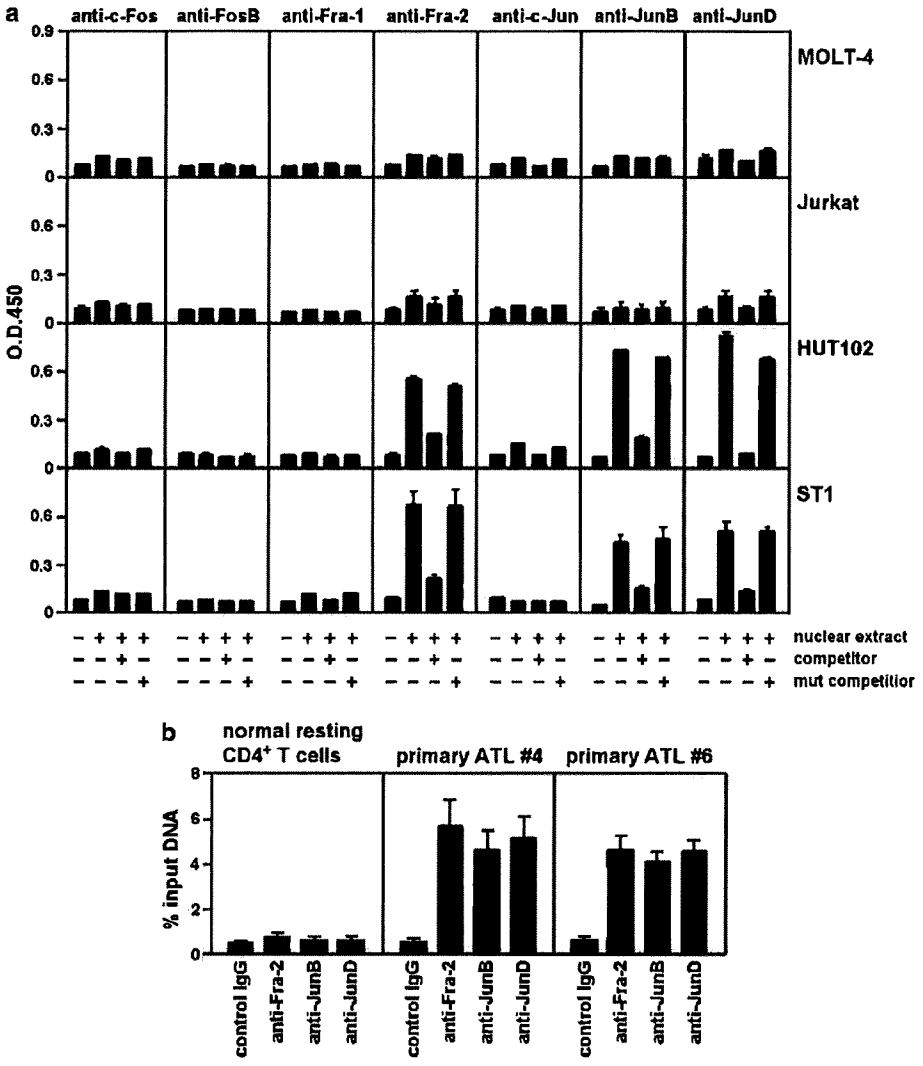

Figure 4 Specific binding of Fra-2, JunB and JunD to the AP-1 site in the CCR4 promoter. (a) NoShift assay. Nuclear extracts were prepared from two control T-cell lines (MOLT-4 and Jurkat) and two adult T-cell leukemia (ATL) cell lines (HUT102 and ST1). Nuclear proteins that bound to the biotinylated AP-1 site oligonucleotide (TGGGAAATGACTAAGAATCAT) were captured on an avidin-coated plate and detected by anti-c-Fos, anti-FosB, anti-Fra-1, anti-Fra-2, anti-c-Jun, anti-JunB or anti-JunD, as indicated. Specificity was determined by adding unlabeled probe (competitor; TGGGAAATGACTAAGAATCAT) or mutant probe (mut competitor; TGGGAAATGTCAAAGAATCAT; differences underlined). Each bar represents the mean ± s.e.m. from three separate experiments. (b) Chromatin immunoprecipitation (ChIP) assay. Chromatins from normal CD4+ T cells from healthy donors (purity, >96%) and primary ATL cells from two patients (leukemic cells, >90%) were immunoprecipitated with anti-Fra-2, anti-JunD or control IgG. The amounts of precipitated DNA relative to total input DNA were quantified by real-time PCR for the CCR4 promoter region containing the AP-1 site. Each bar represents the mean ± s.e.m. from three separate experiments.

Identification of downstream target genes of the Fra-2/JunD heterodimer in ATL cells

To identify the target genes of Fra-2 in ATL cells, we compared the gene expression profiles of ATL-derived ST1 cells transfected with Fra-2 siRNA or control siRNA using the Affymetrix high-density oligonucleotide microarray. As summarized in Figure 6a, at least 49 genes were downregulated more than threefold by Fra-2 siRNA. The classification of these genes according to their biological functions shows that Fra-2 promotes the expression of genes involved in signal transduction (10 genes), protein biosynthesis and modification (8 genes) and transcription (6 genes); it also stimulates the expression of 10 genes of unknown function. Most notably, the list includes the proto-oncogenes c-Myb, BCL-6 and MDM2 (Oh and Reddy, 1999; Pasqualucci *et al*., 2003; Vargas *et al*., 2003). As shown in Figure 6b, RT–PCR analysis verified that not only Fra-2 siRNA but also JunD siRNA downregulated these proto-oncogenes in two ATL cell lines. Therefore, c-Myb, BCL-6 and MDM2 are the downstream target genes of the Fra-2/JunD heterodimer in both cell lines. This prompted us to examine the expression of c-Myb, BCL-6 and MDM2 in freshly isolated primary ATL cells by

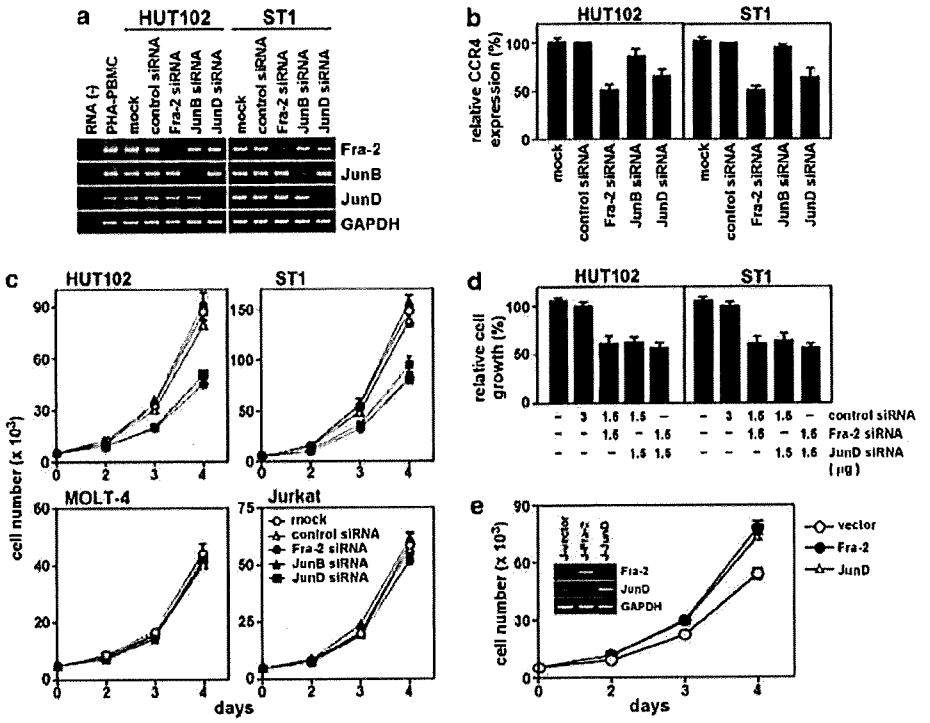

Figure 5 Dominant role of Fra-2/JunD in CCR4 expression and cell proliferation in adult T-cell leukemia (ATL). (a) Reverse transcription (RT)–PCR analysis to determine the effect of siRNAs. HUT102 and ST1 were transfected with control siRNA or siRNA for Fra-2, JunB or JunD. After 48 h, total RNA was prepared. The representative results from three separate experiments are shown. (b) Real-time RT–PCR analysis for CCR4 expression. HUT102 and ST1 were transfected with control siRNA or siRNA for Fra-2, JunB or JunD. After 48 h, total RNA was prepared and real-time RT–PCR was performed for CCR4 and 18S ribosomal RNA (an internal control). Data are presented as the mean ± s.e.m. of three separate experiments. (c) Effect of siRNAs on cell growth. HUT102, ST1, MOLT-4 and Jurkat were transfected with control, Fra-2, JunB and JunD siRNAs and cultured in a 96-well plate at 0.5×10^4 cells per well. At the indicated time points, viable cell numbers were determined using a FACSCalibur by gating out cells stained with propidium iodide. Data are shown as the mean ± s.e.m. of three separate experiments. (d) Effect of double knockdown of Fra-2 and JunD on cell growth. HUT102 and ST1 were transfected with control, Fra-2 and JunD siRNAs as indicated and cultured in a 96-well plate at 0.5×10^4 cells per well. At 4 days, viable cell numbers were determined on a FACSCalibur by gating out dead cells stained with propidium iodide. Data are shown as the mean ± s.e.m. of three separate experiments. (e) Effect of stable expression of Fra-2 and JunD on cell growth. Jurkat cells were transfected with a control IRES-EGFP expression vector or an IRES-EGFP expression vector for Fra-2 or JunD. Stable transfectants expressing green fluorescence protein were sorted and cultured in a 96-well plate at 0.5×10^4 cells per well. At the indicated time points, viable cell numbers were determined on a FACSCalibur by gating out dead cells stained with propidium iodide. Data are shown as the mean ± s.e.m. of three separate experiments.

RT–PCR. As shown in Figure 6c, we indeed detected the constitutive expression of c-Myb, BCL-6 and MDM2 at high levels in primary ATL cells. In sharp contrast, normal resting $CD4^+$ T cells hardly expressed these proto-oncogenes.

Discussion

The AP-1 transcription factors function as homodimers or heterodimers formed by Jun (c-Jun, JunB and JunD), Fos (c-Fos, FosB, Fra-1 and Fra-2) and the ATF family proteins (Shaulian and Karin, 2002; Eferl and Wagner, 2003). Most of them are rapidly and transiently induced by extracellular stimuli that trigger the activation of the Janus kinase (JNK), extracellular signal regulated protein kinases 1 and 2 (ERK1/2) or p38 mitogen-activated protein (MAP) kinase pathways (Shaulian and Karin, 2002; Eferl and Wagner, 2003). The AP-1 family is known to be involved in cellular proliferation, oncogenesis and even tumor suppression, depending on the combination of AP-1 proteins and the cellular context (Shaulian and Karin, 2002; Eferl and Wagner, 2003). Previously, by using the AP-1 site of the IL-8 promoter, Mori *et al.* demonstrated a strong Tax-independent expression of JunD in primary ATL cells (Mori *et al.*, 2000). In the present study, we have shown that Fra-2 is constitutively expressed at high levels in primary ATL cells (Figure 2a). Furthermore, except for JunB and JunD, other members of the AP-1 family are mostly negative in primary ATL cells (Figure 2a). Therefore, as demonstrated in the present study, the Fra-2/JunD and Fra-2/JunB heterodimers may be the major AP-1 factors constitutively active in primary ATL cells.

It has been shown that HTLV-1 Tax induces the expression of various AP-1 family members such as c-Fos, Fra-1, c-Jun and JunD (Nagata *et al.*, 1989; Iwai *et al.*, 2001). We indeed observed the expression of

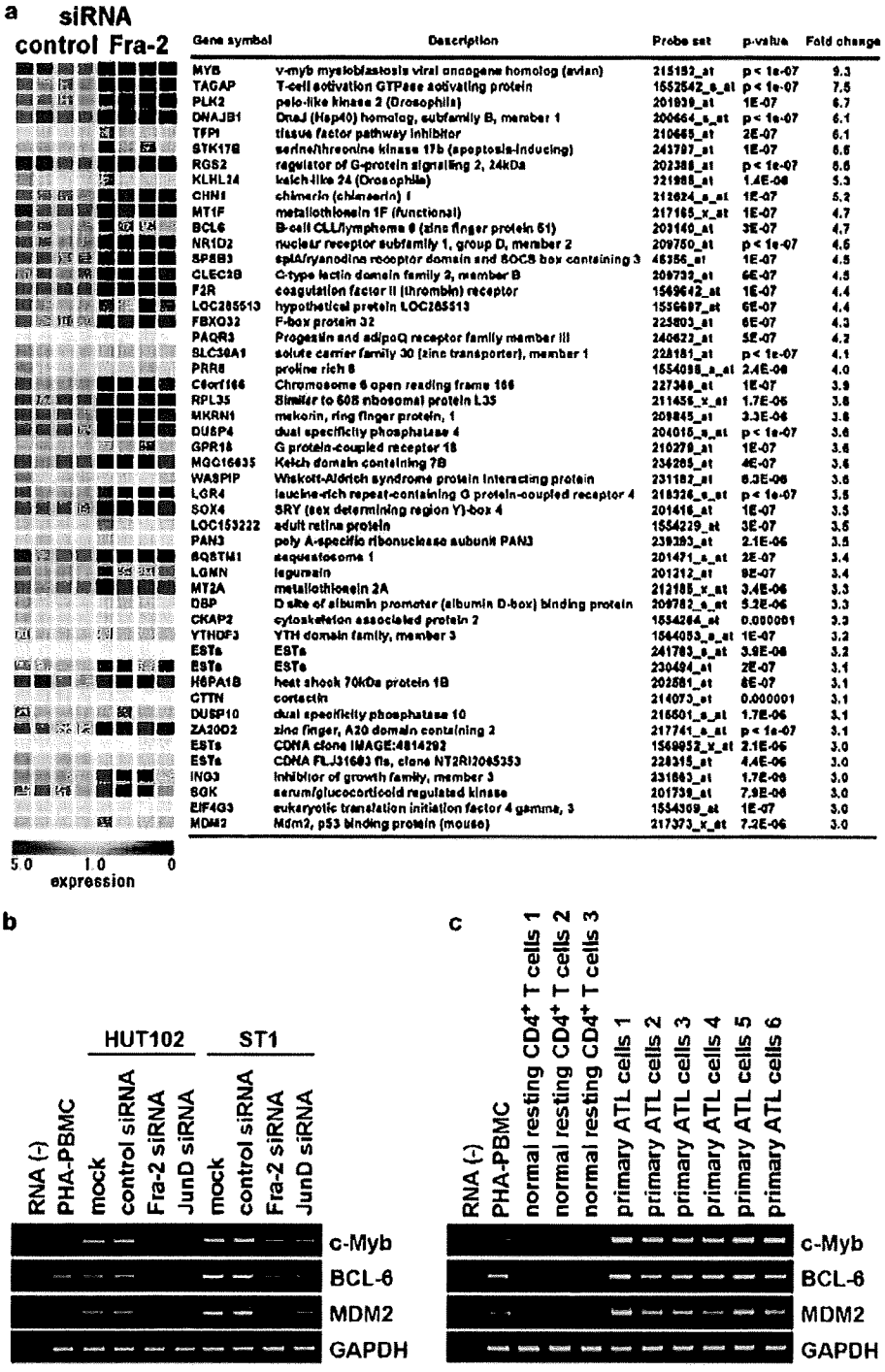

Gene symbol	Description	Probe set	p-value	Fold change
MYB	v-myb myeloblastosis viral oncogene homolog (avian)	215153_at	p < 1e-07	9.3
TAGAP	T-cell activation GTPase activating protein	1552542_a_at	p < 1e-07	7.5
PLK2	polo-like kinase 2 (Drosophila)	201939_at	1E-07	6.7
DNAJB1	DnaJ (Hsp40) homolog, subfamily B, member 1	200664_s_at	p < 1e-07	6.1
TFPI	tissue factor pathway inhibitor	210665_at	2E-07	6.1
STK17B	serine/threonine kinase 17b (apoptosis-inducing)	241787_at	1E-07	6.6
RGS2	regulator of G-protein signalling 2, 24kDa	202388_at	p < 1e-07	6.6
KLHL24	kelch-like 24 (Drosophila)	221988_at	1.4E-06	5.3
CHN1	chimerin (chimaerin) 1	213624_s_at	1E-07	5.2
MT1F	metallothionein 1F (functional)	217165_x_at	1E-07	4.7
BCL6	B-cell CLL/lymphoma 6 (zinc finger protein 51)	203140_at	3E-07	4.7
NR1D2	nuclear receptor subfamily 1, group D, member 2	209750_at	p < 1e-07	4.6
SPSB3	splA/ryanodine receptor domain and SOCS box containing 3	46356_at	1E-07	4.5
CLEC2B	C-type lectin domain family 2, member B	209733_at	6E-07	4.5
F2R	coagulation factor II (thrombin) receptor	1549642_at	1E-07	4.4
LOC285513	hypothetical protein LOC285513	1556697_at	6E-07	4.4
FBXO32	F-box protein 32	225803_at	6E-07	4.3
PAQR3	Progestin and adipoQ receptor family member III	240622_at	5E-07	4.2
SLC30A1	solute carrier family 30 (zinc transporter), member 1	228181_at	p < 1e-07	4.1
PRR6	proline rich 6	1554098_a_at	2.4E-06	4.0
C6orf166	Chromosome 6 open reading frame 166	227369_at	1E-07	3.9
RPL35	Similar to 60S ribosomal protein L35	211456_x_at	1.7E-06	3.8
MKRN1	makorin, ring finger protein, 1	209845_at	3.3E-06	3.8
DUSP4	dual specificity phosphatase 4	204015_s_at	p < 1e-07	3.6
GPR18	G protein-coupled receptor 18	210279_at	1E-07	3.6
MGC16635	Kelch domain containing 7B	234285_at	4E-07	3.6
WASPIP	Wiskott-Aldrich syndrome protein interacting protein	231182_at	6.3E-06	3.6
LGR4	leucine-rich repeat-containing G protein-coupled receptor 4	218326_s_at	p < 1e-07	3.5
SOX4	SRY (sex determining region Y)-box 4	201416_at	1E-07	3.5
LOC153222	adult retina protein	1554219_at	3E-07	3.5
PAN3	poly A-specific ribonuclease subunit PAN3	239293_at	2.1E-06	3.5
SQSTM1	sequestosome 1	201471_s_at	2E-07	3.4
LGMN	legumain	201212_at	9E-07	3.4
MT2A	metallothionein 2A	212185_x_at	3.4E-06	3.3
DBP	D site of albumin promoter (albumin D-box) binding protein	209782_s_at	5.2E-06	3.3
CKAP2	cytoskeleton associated protein 2	1554264_at	0.000001	3.3
YTHDF3	YTH domain family, member 3	1554055_s_at	1E-07	3.2
ESTs	ESTs	241783_s_at	3.9E-06	3.2
ESTs	ESTs	230494_at	2E-07	3.1
HSPA1B	heat shock 70kDa protein 1B	202581_at	6E-07	3.1
CTTN	cortactin	214073_at	0.000001	3.1
DUSP10	dual specificity phosphatase 10	215501_s_at	1.7E-06	3.1
ZA20D2	zinc finger, A20 domain containing 2	217741_s_at	p < 1e-07	3.1
ESTs	CDNA clone IMAGE:4814292	1569952_x_at	2.1E-06	3.0
ESTs	CDNA FLJ31603 fis, clone NT2RI2005253	228315_at	4.4E-06	3.0
ING3	inhibitor of growth family, member 3	231863_at	1.7E-06	3.0
SGK	serum/glucocorticoid regulated kinase	201739_at	7.9E-06	3.0
EIF4G3	eukaryotic translation initiation factor 4 gamma, 3	1554309_at	1E-07	3.0
MDM2	Mdm2, p53 binding protein (mouse)	217373_x_at	7.2E-06	3.0

Figure 6 Identification of downstream target genes of Fra-2 in adult T-cell leukemia (ATL). (**a**) Microarray analysis. ST1 cells were transfected with control siRNA or Fra-2 siRNA. After 48 h, microarray analysis was performed using the Affymetrix GeneChip HG-U133 Plus 2.0 array. Four independent transfection samples were analysed for each group. Each column represents the expression level of a given gene in an individual sample. Red represents increased expression and blue represents decreased expression relative to the normalized expression of the gene across all samples. We computed the statistical significance level for each gene between the Fra-2-knockdown group and the control group with a mean fold change of >3 by the *t*-test ($P<10^{-5}$). (**b**) Reverse transcription (RT)–PCR analysis. HUT102 and ST1 cells were transfected with control siRNA or siRNA for Fra-2 or JunD. After 48 h, the expression of c-Myb, BCL-6, MDM2 and GAPDH was determined by RT–PCR. The representative results from three separate experiments are shown. (**c**) RT–PCR analysis. Normal $CD4^+$ T cells from healthy donors ($n=3$; purity, $>96\%$) and PBMC from ATL patients ($n=6$; leukemic cells, $>90\%$) were examined for the expression of c-Myb, BCL-6 and MDM2 by RT–PCR. The representative results from two separate experiments are shown.

various AP-1 family members in primary ATL cells (patient nos. 1 and 5) and in some ATL cell lines expressing Tax (Figures 2a and b). However, the constitutive expression of Fra-2, JunD and JunB in freshly isolated primary ATL cells and ATL cell lines is apparently independent from Tax expression (Figures 2a and b). This is further supported by the finding that CCR4-expressing HTLV-1-negative CTCL cell lines also constitutively express Fra-2, JunB and JunD at high levels (Figure 2). By using JPX-9, which is a subline of Jurkat carrying the HTLV-1 Tax gene under the control of the metallothionein gene promoter (Nagata *et al.*, 1989), we have also confirmed that Fra-2 is not inducible by Tax (data not shown).

The CCR4 promoter was potently activated by the Fra-2/JunB and Fra-2/JunD heterodimers (Figure 3a). Fra-2, JunB and JunD were also shown to bind specifically to the AP-1 site in the CCR4 promoter *in vitro* by the NoShift binding assays and *in vivo* by the ChIP assays (Figures 4a and b). By using the siRNA knockdown technique, however, only Fra-2 siRNA and JunD siRNA efficiently suppressed CCR4 expression and cell growth in ATL cell lines (Figure 5). On the other hand, JunB siRNA showed little such effect (Figure 5). Therefore, it is likely that, at least in terms of CCR4 expression and cell proliferation, the Fra-2/JunD heterodimer plays a more dominant role than the Fra-2/JunB heterodimer in ATL cells. It thus remains to be determined whether the Fra-2/JunB heterodimer has any specific functions in ATL.

The most striking finding in the present study is the aberrant expression of Fra-2 in primary ATL cells. Fra-2 expression is essentially absent in normal $CD4^+$ T cells under various conditions thus far examined (Figures 2a and c). Physiologically, Fra-2 is known to be expressed by various epithelial cells and in cartilaginous structures and has been shown to be required for efficient cartilage development (Karreth *et al.*, 2004). With regard to lymphoid cells, developing murine thymocytes were reported to express Fra-2 (Chen *et al.*, 1999). Previous studies have shown that individual homodimeric and heterodimeric AP-1 proteins have different functional properties and target genes (Shaulian and Karin, 2002; Eferl and Wagner, 2003). However, little is known about the target genes of Fra-2 and even less is known about the oncogenic role of Fra-2 in human malignancies. In this study, we have shown that CCR4 is the direct target gene of Fra-2 in association with JunD in ATL cells. Furthermore, we have shown that at least 49 genes are downregulated more than threefold in the ATL cell line ST-1 by Fra-2 siRNA (Figure 6). Among these genes, the proto-oncogenes c-Myb, BCL-6 and MDM2 (Oh and Reddy, 1999; Pasqualucci *et al.*, 2003; Vargas *et al.*, 2003) are further confirmed to be dependent on the Fra-2/JunD heterodimer and to be expressed at high levels in primary ATL cells (Figure 6). It remains to be seen whether the Fra-2/JunD heterodimer directly induces these proto-oncogenes or indirectly maintains their expression by promoting cell growth.

c-Myb is the genomic homologue of the avian myeloblastosis virus oncogene v-Myb. c-Myb is widely expressed in immature hematopoietic cells and also in various leukemias and carcinomas (Oh and Reddy, 1999; Shetzline *et al.*, 2004; Hess *et al.*, 2006). The target genes of c-Myb include the anti-apoptotic genes BCL-2 and BCL-X_L and also c-Myc (Ramsay *et al.*, 2003). Thus, c-Myb may promote the survival of ATL cells via BCL-2 and BCL-X_L (Galonek and Hardwick, 2006) and also cell cycle progression via c-Myc (Dang, 1999). BCL-6 was originally identified as the target gene of recurrent chromosomal translocations affecting 3q27 in non-Hodgkin's lymphoma. The expression of BCL-6 is frequently upregulated in diffuse large-cell lymphoma and follicular lymphoma through promoter substitution or somatic promoter point mutations (Ye *et al.*, 1993; Migliazza *et al.*, 1995; Chang *et al.*, 1996). Frequent expression of BCL-6 has also been reported in some T-cell lymphomas (Kerl *et al.*, 2001). The BCL-6 protein has been shown to exert cell-immortalizing and anti-senescence activities (Shvarts *et al.*, 2002; Pasqualucci *et al.*, 2003). Thus, BCL-6 may also inhibit apoptosis and promote cell cycle progression in ATL. The MDM2 protein is a negative regulator of p53 and suppresses p53-mediated cell cycle arrest and apoptosis (Vargas *et al.*, 2003). Elevated expression of MDM2 has been demonstrated in various types of human cancer (Rayburn *et al.*, 2005). Given that only a minor fraction of ATL cases have mutations affecting p53 (Cesarman *et al.*, 1992), the elevated expression of MDM2 may contribute to the functional downregulation of p53 in the majority of ATL cases.

CTCLs are a group of T-cell lymphomas derived from skin-homing memory T cells. CTCLs are not associated with HTLV-1 infection but resemble ATL and frequently express CCR4 (Ferenczi *et al.*, 2002; Kim *et al.*, 2005). Furthermore, CCR4 expression has been shown to be a consistent feature of the large-cell transformation of mycosis fungoides (Jones *et al.*, 2000). In the present study, we have shown that CTCL cell lines also express Fra-2, JunB and JunD at high levels (Figure 2b). Therefore, it is likely that aberrantly expressed Fra-2 in association with Jun proteins, particularly JunD, is also involved in CCR4-expression and cell proliferation in CTCLs.

In conclusion, we have shown that aberrantly expressed Fra-2 in association with JunD is responsible for CCR4 expression in ATL and is also likely to play an important role in ATL oncogenesis in part by inducing the expression of the proto-oncogenes c-Myb, BCL-6 and MDM2. Future studies are necessary to elucidate how the Fra-2/JunD heterodimer induces the expression of these proto-oncogenes and their individual roles in ATL oncogenesis. It also remains to be seen how ATL cells aberrantly express Fra-2 at high levels. Furthermore, the expression and function of Fra-2 in CTCLs remain to be determined.

Materials and methods

Cells

All the human T-cell lines used were described previously (Nagata *et al.*, 1989; Yamada *et al.*, 1996; Hata *et al.*, 1999;

Yoshie *et al.*, 2002). Peripheral blood mononuclear cells (PBMC) were isolated from heparinized blood samples obtained from healthy adult donors and acute ATL patients with a high leukemic cell count (>90%) by using Ficoll-Paque (Amersham Biosciences Corp, Piscataway, NJ, USA). Normal $CD4^+$ T cells (purity, >96%) were further prepared from PBMC by negative selection using an IMagnet system (BD Pharmingen, San Diego, CA, USA). Activated $CD4^+$ T cells were prepared by stimulating $CD4^+$ T cells with anti-CD3 (clone HIT3a; BD Pharmingen) and anti-CD28 (clone CD28.2; BD Pharmingen) for 24 h. The preparation of naive $CD4^+CD45RA^+$ T cells and their polarization into Th1 and Th2 cells were performed as described previously (Imai *et al.*, 1999). Primary ATL cells and normal resting $CD4^+$ T cells were used without culture for the experiments. This study was approved by the local ethical committee and written informed consent was obtained from each patient.

Transfection and luciferase assay

The major transcriptional start site (+1) of the human CCR4 gene was determined by the method of rapid amplification of cDNA 5′-ends and was found to be located 1797 bases upstream from the translation start codon (data not shown). To generate a promoter–reporter construct, the 1-kb promoter region of the human CCR4 gene (−983 to +25) was amplified from the genomic DNA by PCR using primers based on a GenBank genomic DNA sequence (accession no. NC_000003) and inserted into the reporter plasmid pGL3-Basic (Promega, Madison, WI, USA). Deletions and site-directed mutations were also performed using PCR. pGL3-2xAP-1 was constructed by introducing a sequence containing two copies of the AP-1 consensus binding site (TGATGACTCAGCCG-GAATGATGACTCAGCC) in front of a minimal CCR4 promoter pGL3 (−96/+25; Figure 1b). The coding regions of human FosB and GATA-3 were amplified from a cDNA library generated from phytohemagglutinin (PHA)-stimulated PBMC by PCR and cloned into the expression vector pSG5 (Stratagene, La Jolla, CA, USA). The coding region of HTLV-1 HBZ was amplified from a cDNA library generated from the HTLV-1^+ T-cell line C8166 by PCR and cloned into the expression vector pEF4/myc-His A (Invitrogen, Carlsbad, CA, USA). The expression vectors for c-Fos, Fra-1, Fra-2, c-Jun, JunB, JunD and Tax were described previously (Iwai *et al.*, 2001). Cells (5×10^5) were transfected with 2 μg of reporter plasmid, 0.5 μg of expression plasmids for various transcription factors and 1 μg of pSV-β-galactosidase using DMRIE-C (Invitrogen). After 24–27 h, luciferase assays were performed using a Luciferase Assay kit (Promega). Luciferase activity was normalized by β-galactosidase activity that served as an internal control for transfection efficiency.

RT–PCR

RT–PCR was carried out as described previously (Yoshie *et al.*, 2002). The primers used were as follows: +5′-AAGAA GAACAAGGCGGTGAAGATG-3′ and −5′-AGGCCCC TGCAGGTTTTGAAG-3′ for CCR4; +5′-TACTACCACTC ACCCGCAGACTC-3′ and −5′-CTTTTCCCTTCGGATTCT CCTTTT-3′ for c-Fos; +5′-TAGCAGCAGCTAAATGC AGGAAC-3′ and −5′-CCAGCTGAAGCCATCTTCCTT AG-3′ for FosB; +5′-CAGTGGATGGTACAGCCTCA TTT-3′ and −5′-GCCCAGATTTCTCATCTTCCAGT-3′ for Fra-1; +5′-CCAGCAGAAATTCCGGGTAGATA-3′ and −5′-TCTCCTCCTCTTCAGGAGACAGC-3′ for Fra-2; +5′-AAACAGAGCATGACCCTGAACCT-3′ and −5′-CTC CTGCTCATCTGTCACGTTCT-3′ for c-Jun; +5′-AAAAT GGAACAGCCCTTCTACCA-3′ and −5′-AGCCCTGACCA GAAAAGTAGCTG-3′ for JunB; +5′-AACACCCTTCT ACGGCGATGAG-3′ and −5′-GGGTAGAGGAACTGTG AGCTCGT-3′ for JunD; +5′-GAATTGGTGGACGGG CTATTATC-3′ and −5′-TAGCACTATGCTGTTTCGCCT TC-3′ for HBZ; +5′-CCGGCGCTGCTCTCATCCCGGT-3′ and −5′-GGCCGAACATAGTCCCCCAGAG-3′ for Tax; +5′-AAGGCATCCAGACCAGAAACCG-3′ and −5′-AGC ATCGAGCAGGGCTCTAACC-3′ for GATA-3; +5′-CAGT GACGAGGATGATGAGGACT-3′ and −5′-AACGTTTCG GACCGTATTTCTGT-3′ for c-Myb; +5′-ATTCCAGCTT CGGAACAAGAGAC-3′ and −5′-GTCCTTTTGATCAC TCCCACCTT-3′ for MDM2; +5′-CAAGAAGTTTCTAGG AAAGGCCGG-3′ and −5′-GATTGATCACACTAA GGTTGCATT-3′ for BCL-6 and +5′-GCCAAGGTCATCC ATGACAACTTTGG-3′ and −5′-GCCTGCTTCACCA CCTTCTTGATGTC-3′ for glyceraldehyde-3-phosphate dehydrogenase (GAPDH). The amplification conditions were denaturation at 94 °C for 30 s (5 min for the first cycle), annealing at 60 °C for 30 s and extension at 72 °C for 30 s (5 min for the last cycle) for 34 cycles for CCR4; 35 cycles for c-Fos, FosB, Fra-1, Fra-2, c-Jun, JunB, JunD, HBZ, Tax, c-Myb, BCL-6 and MDM2; 29 cycles for GATA-3 and 27 cycles for GAPDH. Amplification products were electrophoretically run on a 2% agarose gel and stained with ethidium bromide.

Quantitative real-time PCR was carried out using the TaqMan assay and a 7700 Sequence Detection System (Applied Biosystems, Foster City, CA, USA). The conditions for PCR were 50 °C for 2 min, 95 °C for 10 min and then 50 cycles of 95 °C for 15 s (denaturation) and 60 °C for 1 min (annealing extension). The primers and fluorogenic probes for CCR4 and 18S ribosomal RNA were obtained from a TaqMan kit (Applied Biosystems). Quantification of CCR4 expression was performed using the Sequence Detector System Software (Applied Biosystems).

NoShift transcription factor assay

Anti-c-Fos (sc-52), anti-FosB (sc-7203), anti-Fra-1 (sc-22794), anti-Fra-2 (sc-604), anti-c-Jun (sc-1694), anti-JunB (sc-73) and anti-JunD (sc-74) were purchased from Santa Cruz Biotechnology (Santa Cruz, CA, USA). Transcription factors bound to specific DNA sequences were identified using the NoShift Transcription Factor Assay Kit (EMD Biosciences, Madison, WI, USA). Nuclear extracts were prepared from human T-cell lines by using the NucBuster Protein Extraction Kit (EMD Biosciences). The oligonucleotides used were as follows (differences underlined): TGGGAAATGACTAAGAATCAT for the biotinylated probe and unlabeled competitor of the AP-1 site and TGGGAAATGTCAAAGAATCAT for the mutated AP-1 site.

ChIP assay

This assay was performed using a ChIP assay kit (Upstate Biotechnology, Lake Placid, NY, USA) following the manufacturer's instructions. In brief, cells (1×10^6) were cross-linked with 1% formaldehyde for 10 min at room temperature. The cell pellets were lysed with sodium dodecyl sulfate (SDS) lysis buffer and sonicated to shear DNA to a size range between 200 and 1000 bp. After centrifugation, the supernatant was diluted 10-fold in ChIP dilution buffer and incubated overnight at 4 °C with 4 μg of anti-Fra-2 (sc-604), anti-JunB (sc-73), anti-JunD (sc-74) or normal rabbit IgG (DAKO, Kyoto, Japan). Immunocomplexes were collected by adding protein A-agarose beads. The immune complexes were incubated at 65 °C for 4 h to reverse the protein/DNA cross-links. DNAs were then purified by phenol/chloroform extraction and used as templates for quantitative real-time PCR. The primers and

the fluorogenic probe for the AP-1 site of the CCR4 promoter were as follows: primers: +5′-GGTCTTGGGAAATGACT AAGAATCA-3′ and −5′-TCTCCCTCACCCAACTGTACT AAGT-3′; probe: 5′-TCTGCTTCCTACTTCTATCAAA AAACCCCACTTG-3′.

Immunological staining
Cells were spotted on a glass slide and fixed with 4% paraformaldehyde. Tissue sections were prepared from formalin-fixed and paraffin-embedded biopsy tissue samples and subjected to microwave irradiation for 5 min three times in Target Retrieval Solution (DAKO). Slides and tissue sections were incubated for 1 h at room temperature with anti-Fra-2 (sc-604), anti-JunB (sc-73), anti-JunD (sc-74) or mouse monoclonal anti-CCR4 (KM-2160; Kyowa Hakko, Tokyo, Japan). Normal rabbit IgG and control mouse IgG_1 (DAKO) were used as negative controls. After washing, the slides and tissue sections were incubated with biotin-labeled goat anti-rabbit IgG or biotin-labeled horse anti-mouse IgG followed by detection using the Vectastain ABC/HRP kit (Vector Laboratories, Burlingame, CA, USA). Finally, cells and sections were counterstained with Gill's hematoxylin (Polysciences, Warrington, PA, USA), dehydrated and mounted.

Transfection of siRNA
siRNAs for Fra-2 (SI00420455), JunB (SI03077445), JunD (SI00075985) and the negative control (1022064) were obtained from Qiagen (Hilden, Germany). Transfection experiments were performed using Amaxa Nucleofector (Amaxa, Cologne, Germany). Cells (1×10^6) were resuspended in 100 µl of Nucleofector solution (T solution for MOLT-4, HUT102 and ST1 and V solution for Jurkat) and transfected with 2.5 µg of siRNA using program O-17 for MOLT-4, HUT102 and ST1 and program S-18 for Jurkat. The transfection efficiency was ~95% as determined using fluorescent siRNA (Qiagen).

Cell proliferation assay
Cells were seeded in a 96-well plate at a density of 0.5×10^4 per well and cultured. The number of viable cells was determined every 24 h on a FACSCalibur system (Becton Dickinson, Mountain View, CA, USA) by gating out cells stained with propidium iodide. To prepare stable transfectants of Fra-2 and JunD, the coding regions of human Fra-2 and JunD were inserted into the pIRES2-EGFP vector (BD Biosciences, San Diego, CA, USA). Jurkat cells were transfected with the plasmids using DMRIE-C (Invitrogen). Stable transfectants expressing green fluorescence protein were sorted by flow cytometry using FACSVantage (Becton Dickinson).

Oligonucleotide microarray
Microarray analysis was performed as described previously (Igarashi *et al.*, 2007) using the Affymetrix GeneChip HG-U133 Plus 2.0 array (Affymetrix, Santa Clara, CA, USA). In brief, the ATL-derived cell line ST1 was transfected with control siRNA or Fra-2 siRNA. Four independent transfections were performed for each group. After 48 h, total RNA samples were prepared and confirmed to be of good quality with the Agilent 2100 Bioanalyzer (Agilent Technologies, Waldbronn, Germany). All microarray data have been submitted to the Gene Expression Omnibus (GEO; http://www.ncbi.nlm.nih.gov/geo; accession no. GSE6379). The analysis was performed using the BRB Array Tools software version 3.3.0 (http://linus.nci.nih.gov/BRB-ArrayTools.html) developed by Richard Simon and Amy Peng.

Acknowledgements

We thank Namie Sakiyama for her excellent technical assistance. We also thank Dr Rich Simon and Dr Amy Peng for providing the BRB ArrayTools software. This work was supported in part by a Grant-in-Aid from the Ministry of Education, Culture, Sports and Technology, Japan; by Solution-Oriented Research for Science and Technology (SORST) from Japan Science and Technology Corporation and by High-Tech Research Center Project for Private Universities: matching fund subsidy from the Ministry of Education, Culture, Sports, Science and Technology of Japan, 2002–2009.

References

Basbous J, Arpin C, Gaudray G, Piechaczyk M, Devaux C, Mesnard JM. (2003). The HBZ factor of human T-cell leukemia virus type I dimerizes with transcription factors JunB and c-Jun and modulates their transcriptional activity. *J Biol Chem* **278**: 43620–43627.

Cesarman E, Chadburn A, Inghirami G, Gaidano G, Knowles DM. (1992). Structural and functional analysis of oncogenes and tumor suppressor genes in adult T-cell leukemia/lymphoma shows frequent p53 mutations. *Blood* **80**: 3205–3216.

Chang CC, Ye BH, Chaganti RS, Dalla-Favera R. (1996). BCL-6, a POZ/zinc-finger protein, is a sequence-specific transcriptional repressor. *Proc Natl Acad Sci USA* **93**: 6947–6952.

Chen F, Chen D, Rothenberg EV. (1999). Specific regulation of fos family transcription factors in thymocytes at two developmental checkpoints. *Int Immunol* **11**: 677–688.

Dang CV. (1999). c-Myc target genes involved in cell growth, apoptosis, and metabolism. *Mol Cell Biol* **19**: 1–11.

Eferl R, Wagner EF. (2003). AP-1: a double-edged sword in tumorigenesis. *Nat Rev Cancer* **3**: 859–868.

Ferenczi K, Fuhlbrigge RC, Pinkus J, Pinkus GS, Kupper TS. (2002). Increased CCR4 expression in cutaneous T cell lymphoma. *J Invest Dermatol* **119**: 1405–1410.

Galonek HL, Hardwick JM. (2006). Upgrading the BCL-2 Network. *Nat Cell Biol* **8**: 1317–1319.

Grassmann R, Aboud M, Jeang KT. (2005). Molecular mechanisms of cellular transformation by HTLV-1 Tax. *Oncogene* **24**: 5976–5985.

Hata T, Fujimoto T, Tsushima H, Murata K, Tsukasaki K, Atogami S *et al.* (1999). Multi-clonal expansion of unique human T-lymphotropic virus type-I-infected T cells with high growth potential in response to interleukin-2 in prodromal phase of adult T cell leukemia. *Leukemia* **13**: 215–221.

Hess JL, Bittner CB, Zeisig DT, Bach C, Fuchs U, Borkhardt A *et al.* (2006). c-Myb is an essential downstream target for homeobox-mediated transformation of hematopoietic cells. *Blood* **108**: 297–304.

Hori S, Nomura T, Sakaguchi S. (2003). Control of regulatory T cell development by the transcription factor Foxp3. *Science* **299**: 1057–1061.

Iellem A, Mariani M, Lang R, Recalde H, Panina-Bordignon P, Sinigaglia F *et al.* (2001). Unique chemotactic response profile and specific expression of chemokine receptors CCR4 and CCR8 by CD4(+)CD25(+) regulatory T cells. *J Exp Med* **194**: 847–853.

Igarashi T, Izumi H, Uchiumi T, Nishio K, Arao T, Tanabe M *et al.* (2007). Clock and ATF4 transcription system regulates drug resistance in human cancer cell lines. *Oncogene* **26**: 4749–4760.

Imai T, Nagira M, Takagi S, Kakizaki M, Nishimura M, Wang J *et al.* (1999). Selective recruitment of CCR4-bearing Th2 cells toward antigen-presenting cells by the CC chemokines thymus and

activation-regulated chemokine and macrophage-derived chemokine. *Int Immunol* **11**: 81–88.

Ishida T, Utsunomiya A, Iida S, Inagaki H, Takatsuka Y, Kusumoto S *et al.* (2003). Clinical significance of CCR4 expression in adult T-cell leukemia/lymphoma: its close association with skin involvement and unfavorable outcome. *Clin Cancer Res* **9**: 3625–3634.

Iwai K, Mori N, Oie M, Yamamoto N, Fujii M. (2001). Human T-cell leukemia virus type 1 tax protein activates transcription through AP-1 site by inducing DNA binding activity in T cells. *Virology* **279**: 38–46.

Jeang KT, Chiu R, Santos E, Kim SJ. (1991). Induction of the HTLV-I LTR by Jun occurs through the Tax-responsive 21-bp elements. *Virology* **181**: 218–227.

Jones D, O C, Kraus MD, Perez-Atayde AR, Shahsafaei A, Wu L *et al.* (2000). Expression pattern of T-cell-associated chemokine receptors and their chemokines correlates with specific subtypes of T-cell non-Hodgkin lymphoma. *Blood* **96**: 685–690.

Karreth F, Hoebertz A, Scheuch H, Eferl R, Wagner EF. (2004). The AP1 transcription factor Fra2 is required for efficient cartilage development. *Development* **131**: 5717–5725.

Karube K, Ohshima K, Tsuchiya T, Yamaguchi T, Kawano R, Suzumiya J *et al.* (2004). Expression of FoxP3, a key molecule in CD4CD25 regulatory T cells, in adult T-cell leukaemia/lymphoma cells. *Br J Haematol* **126**: 81–84.

Kerl K, Vonlanthen R, Nagy M, Bolzonello NJ, Gindre P, Hurwitz N *et al.* (2001). Alterations on the 5′ noncoding region of the BCL-6 gene are not correlated with BCL-6 protein expression in T cell non-Hodgkin lymphomas. *Lab Invest* **81**: 1693–1702.

Kim EJ, Hess S, Richardson SK, Newton S, Showe LC, Benoit BM *et al.* (2005). Immunopathogenesis and therapy of cutaneous T cell lymphoma. *J Clin Invest* **115**: 798–812.

Matsubara Y, Hori T, Morita R, Sakaguchi S, Uchiyama T. (2005). Phenotypic and functional relationship between adult T-cell leukemia cells and regulatory T cells. *Leukemia* **19**: 482–483.

Matsuoka M. (2003). Human T-cell leukemia virus type I and adult T-cell leukemia. *Oncogene* **22**: 5131–5140.

Migliazza A, Martinotti S, Chen W, Fusco C, Ye BH, Knowles DM *et al.* (1995). Frequent somatic hypermutation of the 5′ noncoding region of the BCL6 gene in B-cell lymphoma. *Proc Natl Acad Sci USA* **92**: 12520–12524.

Mori N, Fujii M, Ikeda S, Yamada Y, Tomonaga M, Ballard DW *et al.* (1999). Constitutive activation of NF-kappaB in primary adult T-cell leukemia cells. *Blood* **93**: 2360–2368.

Mori N, Fujii M, Iwai K, Ikeda S, Yamasaki Y, Hata T *et al.* (2000). Constitutive activation of transcription factor AP-1 in primary adult T-cell leukemia cells. *Blood* **95**: 3915–3921.

Nagakubo D, Jin Z, Hieshima K, Nakayama T, Shirakawa AK, Tanaka Y *et al.* (2007). Expression of CCR9 in HTLV-1$^+$ T cells and ATL cells expressing Tax. *Int J Cancer* **120**: 1591–1597.

Nagata K, Ohtani K, Nakamura M, Sugamura K. (1989). Activation of endogenous c-fos proto-oncogene expression by human T-cell leukemia virus type I-encoded p40tax protein in the human T-cell line, Jurkat. *J Virol* **63**: 3220–3226.

Oh IH, Reddy EP. (1999). The myb gene family in cell growth, differentiation and apoptosis. *Oncogene* **18**: 3017–3033.

Pasqualucci L, Bereschenko O, Niu H, Klein U, Basso K, Guglielmino R *et al.* (2003). Molecular pathogenesis of non-Hodgkin's lymphoma: the role of Bcl-6. *Leuk Lymphoma* **44**(Suppl 3): S5–S12.

Ramsay RG, Barton AL, Gonda TJ. (2003). Targeting c-Myb expression in human disease. *Expert Opin Ther Targets* **7**: 235–248.

Rayburn E, Zhang R, He J, Wang H. (2005). MDM2 and human malignancies: expression, clinical pathology, prognostic markers, and implications for chemotherapy. *Curr Cancer Drug Targets* **5**: 27–41.

Rengarajan J, Szabo SJ, Glimcher LH. (2000). Transcriptional regulation of Th1/Th2 polarization. *Immunol Today* **21**: 479–483.

Satou Y, Yasunaga J, Yoshida M, Matsuoka M. (2006). HTLV-I basic leucine zipper factor gene mRNA supports proliferation of adult T cell leukemia cells. *Proc Natl Acad Sci USA* **103**: 720–725.

Shaulian E, Karin M. (2002). AP-1 as a regulator of cell life and death. *Nat Cell Biol* **4**: E131–E136.

Shetzline SE, Rallapalli R, Dowd KJ, Zou S, Nakata Y, Swider CR *et al.* (2004). Neuromedin U: a Myb-regulated autocrine growth factor for human myeloid leukemias. *Blood* **104**: 1833–1840.

Shvarts A, Brummelkamp TR, Scheeren F, Koh E, Daley GQ, Spits H *et al.* (2002). A senescence rescue screen identifies BCL6 as an inhibitor of anti-proliferative p19(ARF)-p53 signaling. *Genes Dev* **16**: 681–686.

Thebault S, Basbous J, Hivin P, Devaux C, Mesnard JM. (2004). HBZ interacts with JunD and stimulates its transcriptional activity. *FEBS Lett* **562**: 165–170.

Vargas DA, Takahashi S, Ronai Z. (2003). Mdm2: a regulator of cell growth and death. *Adv Cancer Res* **89**: 1–34.

Yamada Y, Ohmoto Y, Hata T, Yamamura M, Murata K, Tsukasaki K *et al.* (1996). Features of the cytokines secreted by adult T cell leukemia (ATL) cells. *Leuk Lymphoma* **21**: 443–447.

Yamamoto N, Hinuma Y. (1985). Viral aetiology of adult T-cell leukaemia. *J Gen Virol* **66**: 1641–1660.

Ye BH, Lista F, Lo Coco F, Knowles DM, Offit K, Chaganti RS *et al.* (1993). Alterations of a zinc finger-encoding gene, BCL-6, in diffuse large-cell lymphoma. *Science* **262**: 747–750.

Yoshida M. (2001). Multiple viral strategies of HTLV-1 for dysregulation of cell growth control. *Annu Rev Immunol* **19**: 475–496.

Yoshie O, Fujisawa R, Nakayama T, Harasawa H, Tago H, Izawa D *et al.* (2002). Frequent expression of CCR4 in adult T-cell leukemia and human T-cell leukemia virus type 1-transformed T cells. *Blood* **99**: 1505–1511.

Yoshie O, Imai T, Nomiyama H. (2001). Chemokines in immunity. *Adv Immunol* **78**: 57–110.

nature medicine

RPN2 gene confers docetaxel resistance in breast cancer

Kimi Honma[1,2], Kyoko Iwao-Koizumi[3], Fumitaka Takeshita[1], Yusuke Yamamoto[1], Teruhiko Yoshida[4], Kazuto Nishio[5], Shunji Nagahara[6], Kikuya Kato[3] & Takahiro Ochiya[1]

Drug resistance acquired by cancer cells has led to treatment failure. To understand the regulatory network underlying docetaxel resistance in breast cancer cells and to identify molecular targets for therapy, we tested small interfering RNAs (siRNAs) against 36 genes whose expression was elevated in human nonresponders to docetaxel for the ability to promote apoptosis of docetaxel-resistant human breast cancer cells (MCF7-ADR cells). The results indicate that the downregulation of the gene encoding ribophorin II (RPN2), which is part of an *N*-oligosaccharyl transferase complex, most efficiently induces apoptosis of MCF7-ADR cells in the presence of docetaxel. RPN2 silencing induced reduced glycosylation of the P-glycoprotein, as well as decreased membrane localization, thereby sensitizing MCF7-ADR cells to docetaxel. Moreover, *in vivo* delivery of siRNA specific for *RPN2* markedly reduced tumor growth in two types of models for drug resistance. Thus, RPN2 silencing makes cancer cells hypersensitive response to docetaxel, and RPN2 might be a new target for RNA interference–based therapeutics against drug resistance.

Breast cancer is the most common malignancy in women. Either neoadjuvant or adjuvant chemotherapy administered to subjects with stage 1–3 breast cancers can improve their survival rates[1–3]. Among chemotherapeutic agents, docetaxel, which belongs to the group of taxanes (mitotic inhibitors and antimicrotubule agents), has been shown to have well-established benefits in breast cancer[4]. The response rate to docetaxel, however, is 50% even in first-line chemotherapy, and it decreases to 20–30% in second- or third-line chemotherapy[5–7]; nearly half of the treated subjects do not respond to it and suffer side effects. There is currently no method to reliably predict tumor responses to docetaxel before therapy or to detect when resistance or hypersensitivity develops. Therefore, the identification of molecular biomarkers in docetaxel-resistant breast cancer that could help in a more accurate assessment of individual treatment and the development of molecular-target therapies that could lead to better tumor reduction are of considerable interest.

It has been reported that the expression of the multidrug transporter P-glycoprotein, encoded by the *MDR1* gene (official gene symbol *ABCB1*), is one of the causes of clinical drug resistance to taxanes[8,9]. Other molecules, such as the multidrug resistance–associated protein MRP1[10,11], breast cancer resistance protein (*ABCG2*) and other transporters[12], which act as energy-dependent efflux pumps capable of expelling a large range of xenobiotics, and GSTpi, which is one of the isoenzymes of the glutathione-*S*-transferase (GST)[13–15], have been extensively reported to be overexpressed in tumor cells showing the multidrug-resistant phenotype. It was recently shown that high thioredoxin expression is associated with resistance to docetaxel in breast cancer[16,17]. These molecules might be clinically useful in the prediction of a response to anticancer drugs. Currently, however, none have proven to be specific target molecules for increasing the efficacy of chemotherapy in breast cancer.

To better understand the regulatory network underlying docetaxel resistance in breast cancer cells and to identify molecular targets for therapy, we initiated gene expression profiling of 44 subjects with breast tumors (22 responders and 22 nonresponders) by adaptor-tagged competitive PCR[18] to identify the genes capable of predicting a docetaxel response in human breast cancer and reported the preliminary results of 85 genes whose expression potentially correlated with docetaxel resistance[16]. In the current study, we used an atelocollagen-based siRNA cell transfection array[19,20] to identify the genes responsible for conferring drug resistance. Among the siRNAs targeting genes that were elevated in nonresponders to docetaxel, siRNA designed for *RPN2* (RNP2 siRNA) significantly promoted docetaxel-dependent apoptosis and cell growth inhibition of MCF7-ADR human breast cancer cells that are resistant to docetaxel. Furthermore, atelocollagen-mediated *in vivo* delivery of RPN2 siRNA significantly reduced drug-resistant tumor growth in mice given docetaxel. RPN2 confers drug resistance via the glycosylation of P-glycoproteins and regulates antiapoptotic genes. Thus, RPN2 siRNA introduction hypersensitizes cancer cell response to chemotherapeutic agents, making RPN2 a potential key target for future RNA interference (RNAi)-based therapeutics against a drug-resistant tumor.

[1]Section for Studies on Metastasis, Japanese National Cancer Center Research Institute, 1-1, Tsukiji, 5-chome, Chuo-ku, Tokyo 104-0045, Japan. [2]Koken Bioscience Institute, KOKEN, 2-13-10 Ukima, Kita-ku, Tokyo 115-0051, Japan. [3]Research Institute, Osaka Medical Center for Cancer and Cardiovascular Diseases, 1-3-2 Nakamichi, Higashinari-ku, Osaka 537-8511, Japan. [4]Genetics Division and [5]Pharmaceutical Division, Japanese National Cancer Center Research Institute, 1-1, Tsukiji, 5-chome, Chuo-ku, Tokyo 104-0045, Japan. [6]Dainippon Sumitomo Pharma, 3-45, Kurakakiuchi, 1-chome, Ibaraki, Osaka 567-0878, Japan. Correspondence should be addressed to T.O. (tochiya@ncc.go.jp).

Received 2 March; accepted 10 July; published online 17 August 2008; doi:10.1038/nm.1858

RESULTS

RNAi-based screening for identification of molecular target

As an extension of our previous strategy of analyzing docetaxel resistance in breast cancer cells and of identifying molecular targets for therapy[16], we conducted a study of RNAi-induced gene knockdown in docetaxel-resistant MCF7-ADR human breast cancer cells. Among the 85 genes listed[16], 61 genes that are potentially targets for siRNA strategy were upregulated in human nonresponders. We selected 36 genes with more than a 0.365 signal-to-noise ratio and successfully designed and synthesized siRNAs specific to these genes (**Table 1**). The siRNAs were conjugated to atelocollagen and arrayed on a 96-well microplate. Then, MCF7-ADR cells expressing the luciferase gene (MCF7-ADR-Luc) were seeded into the microplate (the target validation process by cell transfection array is schematically shown in **Supplementary Fig. 1** online.). To evaluate the efficiency of the atelocollagen-mediated cell transfection array, we used GL3 siRNA against the gene encoding luciferase. Atelocollagen-mediated GL3 siRNA delivery caused an approximate 75% reduction of the luciferase activity in MCF7-ADR-Luc cells relative to the control nontargeting siRNA (data not shown). To identify the genes responsible for docetaxel resistance, we assessed siRNAs for their ability to inhibit cell growth and induce apoptosis in the presence of docetaxel compared with the control nontargeting siRNA. We measured cell growth by luciferase activity and examined apoptosis by caspase-7 activation. The results indicated that the downregulation of eight genes (*PTPLB, GSTP1, TUBB, RPN2, SQRDL, NDUFS3, PDCD5* and *MRPL17*) resulted in marked inhibition of cell growth ($P < 0.05$, **Fig. 1a**). Induction of apoptosis was evidenced in cells by downregulation of six genes (*PTPLB, APRT, CFL1, RPN2, SQRDL* and *MRPL17*; $P < 0.05$, **Fig. 1b**). In particular, RPN2 siRNA strongly enhanced caspase-7 activity in the presence of docetaxel ($P < 0.001$, **Supplementary Fig. 2a** online). We validated these results by counting Hoechst-stained cells showing apoptotic nuclear condensation and fragmentation (**Fig. 2a**) and found that there was a significantly higher apoptotic cell death rate in cells given RPN2 siRNA and docetaxel relative to that in cells given RPN2 siRNA alone ($P < 0.02$, **Fig. 2b**). No significant difference was observed in cells with nontargeting control siRNA (**Fig. 2b**). At 72 h after treatment with siRNA and docetaxel, there was substantial cell death induced by RPN2 siRNA compared with the control nontargeting siRNA (**Fig. 2c**). At 96 h after the transfection, almost all RPN2 siRNA–treated cells were detached and disappeared from the culture dishes.

Table 1 The list of 36 genes whose expression is elevated in nonresponders to docetaxel in subjects with breast cancer

No	Gene	Description	Accession number
1	*UFM1*	Ubiquitin-fold modifier 1	BC005193
2	*PTPLB*	Protein tyrosine phosphatase-like (proline instead of catalytic arginine), member b	AF052159
3	*S100A10*	S100 calcium binding protein A10	M38591
4	*APRT*	Adenine phosphoribosyltransferase	Y00486
5	*CFL1*	Cofilin-1 (non-muscle)	X95404
6	*GSTP1*	Glutathione *S*-transferase pi 1	M24485
7	*HSPA5*	Heat shock 70 kDa protein 5 (glucose-regulated protein, 78 kDa)	M19645
8	*GNB2L1*	Guanine nucleotide binding protein (G protein), β polypeptide 2 like 1	M24194
9	*TUBB*	Tubulin, β	BC001002
10	*MX1*	Myxovirus (influenza virus) resistance 1, interferon-inducible protein p78 (mouse)	M33882
11	*COX7C*	Cytochrome *c* oxidase subunit VIIc	BC001005
12	*RPN2*	Ribophorin II	Y00282
13	*DYNLL1*	Dynein, light chain, LC8-type 1	U32944
14	*FXR1*	Fragile X mental retardation, autosomal homolog 1	U25165
15	*SQRDL*	Sulfide quinone reductase-like (yeast)	AF151802
16	*NDUFS3*	NADH dehydrogenase (ubiquinone) Fe-S protein 3, 30 kDa (NADH-coenzyme Q reductase)	AL135819
17	*EST*	ESTs	AL358933
18	*C19orf10*	Chromosome 19 open reading frame 10	BC003639
19	*ATP5E*	ATP synthase, H^+ transporting, mitochondrial F1 complex, ε subunit	AF052955
20	*PDCD5*	Programmed cell death 5	AF014955
21	*CLPTM1L*	CLPTM1-like	AL137440
22	*PPP1R14B*	Protein phosphatase 1, regulatory (inhibitor) subunit 14B	X91195
23	*MRPL17*	Mitochondrial ribosomal protein L17	AK026857
24	*TUBA1B*	Tubulin, α1b	BC006481
25	*IFI6*	Interferon, α-inducible protein 6	X02492
26	*GAPDH*	Glyceraldehyde-3-phosphate dehydrogenase	AF261085
27	*SLC25A3*	Solute carrier family 25 (mitochondrial carrier; phosphate carrier), member 3	BC006455
28	*MAD2L2*	MAD2 mitotic arrest deficient-like 2 (yeast)	AF157482
29	*CTNNB1*	Catenin (cadherin-associated protein), β1, 88 kDa	X87838
30	*CALR*	Calreticulin	M84739
31	*MRPS6*	Mitochondrial ribosomal protein S6	BC000547
32	*ANGPTL2*	Angiopoietin-like 2	AF007150
33	*RPL38*	Ribosomal protein L38	Z26876
34	*ANAPC7*	Anaphase promoting complex subunit 7	AY007104
35	*ENO1*	Enolase 1, (α)	BC004325
36	*ALDH2*	Aldehyde dehydrogenase 2 family (mitochondrial)	M20456

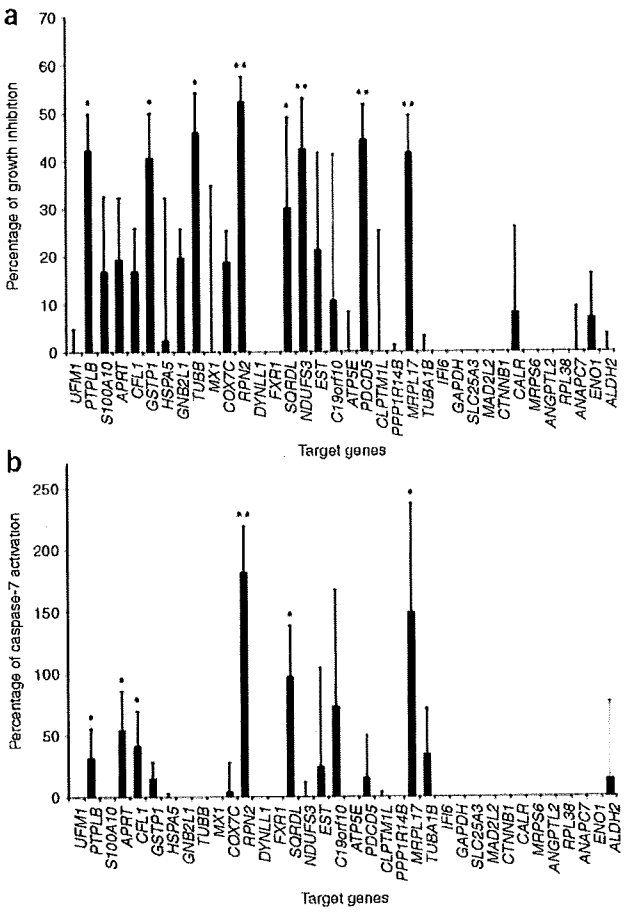

Figure 1 RNAi cell transfection array analysis in cultured breast cancer cells. **(a)** Inhibition of cell growth by 36 siRNAs on atelocollagen-based cell transfection arrays in the presence of docetaxel (1 nM) 72 h after transfection. The cell growth was estimated by luciferase activity in MCF7-ADR-Luc cells, which stably express luciferase ($n = 4$ per group; $^*P < 0.05$, $^{**}P < 0.01$). **(b)** Activation of caspase-7 by 36 siRNAs on atelocollagen-based cell transfection arrays in the presence of docetaxel (1 nM) 72 h after transfection. After the detection of luciferase activity, the same cell transfection arrays were assigned to the measurement of caspase-7 activity, which is elevated in apoptotic MCF7-ADR-Luc cells ($n = 4$ per group; $^*P < 0.05$, $^{**}P < 0.01$). Values are means ± s.d.

However, the expression of other genes was also found to correlate with docetaxel resistance by RNAi-based screening, and they could have some possible additive or synergistic effects with RPN2. Thus, we examined the induction of apoptosis after cotransfection of RPN2 siRNA and siRNAs against other genes that caused cell growth inhibition, apoptosis induction or both in docetaxel-resistant MC7-ADR cells. Knockdown of *PTPLB*, *APRT*, *CFL1*, *GSTP1*, *TUBB*, *SQRDL*, *NDUFS3*, *PDCD5* or *MRPL17* genes with simultaneous knockdown of *RPN2* did not significantly enhance caspase-7 activity relative to the knockdown of *RPN2* alone (**Supplementary Fig. 2b**). This result shows that knockdown of the other genes does not have an additive effect when used together with knockdown of RPN2.

We confirmed the efficacy of RPN2 siRNA for the knockdown of RPN2 messenger RNA by cell-direct real-time RT-PCR analysis. This analysis revealed that RPN2 siRNA inhibited 80% of the mRNA level relative to the control nontargeting siRNA (**Fig. 2d**). Immunofluorescence staining of the RPN2 protein revealed that the RPN2 protein localized in the cytoplasm and its expression was decreased by RPN2 siRNA (**Fig. 2e**). In further experiments, a liposome-mediated RPN2 siRNA transfection was performed. The western blot analysis showed a 45% reduction in RPN2 protein abundance (90% reduction of mRNA by real-time RT-PCR analysis) by RPN2 siRNA transfection in comparison with the control nontargeting siRNA (**Fig. 2f**). These results suggest that downregulation of RPN2 expression by siRNA inhibits cell growth and induces apoptosis in the presence of docetaxel.

In addition, we established stable clones expressing short hairpin RNA (shRNA) against RPN2 (shRNP2) and examined the effect on apoptosis induction in MCF7-ADR cells. The clone that expressed the lowest RPN2 mRNA level showed a 70% reduction of RPN2 expression relative to the control clone ($P < 0.001$, **Supplementary Fig. 2c**), and this shRPN2 clone showed a high caspase-7 activity as compared to the control clone in the presence of docetaxel ($P < 0.001$, **Supplementary Fig. 2d**). We examined seven independent clones and found that they all showed a similar phenotype of increasing drug sensitivity (data not shown). Therefore, consistent with our results with synthetic RPN2 siRNA, the data from the shRPN2 experiments provide evidence for the involvement of RPN2 in drug resistance.

To evaluate the effect of RPN2 siRNA on the drug response of MCF7-ADR cells, we measured the half-maximal inhibitory concentration (IC_{50}) for taxanes. The IC_{50} values for docetaxel in MCF7 and MCF7-ADR cells were 9.48 ± 1.48 nM and 40.22 ± 5.14 nM, respectively ($P < 0.001$). RPN2 siRNA–transfected MCF7-ADR cells were 3.5-fold more sensitive to docetaxel compared with nontargeting siRNA–transfected cells (IC_{50} of 11.47 ± 1.97 nM versus 39.48 ± 2.98 nM, $P < 0.001$). Thus, RPN2 silencing makes MCF7-ADR cells sensitive to docetaxel to a degree similar to that in drug-sensitive MCF7 cells. For paclitaxel, another taxane, the IC_{50} values in MCF7 and MCF7-ADR cells were 13.00 ± 2.02 nM and 89.74 ± 3.43 nM, respectively ($P < 0.001$). RPN2 siRNA–transfected MCF7-ADR cells were 2.6-fold more sensitive to paclitaxel compared with nontargeting siRNA–transfected cells (IC_{50} of 32.92 ± 3.89 nM versus 84.39 ± 5.48 nM, $P < 0.001$). These results indicate that RPN2 silencing bestows a hypersensitive response to taxanes to drug-resistant breast cancer cells.

In addition, we examined docetaxel-resistant EMT6/AR10.0 cells with high expression of the mouse *Rpn2* gene and the *Mdr1* (*Abcb1b*) and *Mdr3* (*Abcb1a*) genes, which reportedly have a similar role in drug resistance to that of the *MDR1* gene in humans, to see whether they have a similar phenotype to MCF7-ADR cells in terms of RPN2 expression status and drug resistance. The siRNA-mediated knockdown of mouse Rpn2 (70% reduction of mRNA by real-time RT-PCR analysis) significantly induced apoptosis of cells in the presence of docetaxel (**Supplementary Fig. 2e–g**). In contrast, nontargeting control siRNA showed no effect (**Supplementary Fig. 2e–g**). Therefore, these results suggest that RPN2 confers docetaxel resistance to both human and mouse cell lines.

Induction of RPN2 expression by docetaxel treatment

Real-time RT-PCR analysis showed that docetaxel-resistant MCF7-ADR cells expressed a slightly increased level of RPN2 mRNA (approximately 20%, $P < 0.01$) relative to parental MCF7 cells (**Fig. 3a**). However, RPN2 mRNA expression in parental MCF7 cells was markedly induced by docetaxel in a dose-dependent manner at

48 h after treatment (**Fig. 3b**). These data indicate that RPN2 mRNA induction may correlate with the observed antiapoptotic phenotype of MCF7-ADR cells.

Furthermore, MCF7-ADR cells expressed abundant MDR1 mRNA, which is a major cause of docetaxel resistance, whereas docetaxel-sensitive MCF7 cells did not (**Fig. 3c**). Additionally, MDR1 mRNA expression in MCF7 cells was strongly induced by docetaxel at 48 h after treatment (**Fig. 3d**). Together, these data provide a new insight into the development of docetaxel resistance in MCF7 cells: when breast cancer cells coordinately express a high amount the of *MDR1* and *RPN2* gene products, the cells become drug-resistant.

RPN2 expression associates with response to docetaxel

In this study, subjects with breast cancer with complete response and partial response were defined as responders, whereas subjects with no change and progressive disease were defined as nonresponders, in accordance with World Health Organization criteria[16] (**Supplementary Note** online).

Of the 44 subjects, 22 showed a pathologic response to docetaxel, and the other 22 showed no response[16]. To understand the clinical importance of the status of RPN2 expression in the subjects, we compared the expression level (signal log ratio) for RPN2 transcript between nonresponder and responder subjects by the Mann-Whitney *U*-test. The subjects with higher RPN2 expression showed a significantly lower response rate to docetaxel than did those with relatively low expression of RPN2 (signal log ratio expressed as mean ± s.e.m. in nonresponders was 0.347 ± 0.062 versus 0.111 ± 0.052 in responders; $P = 0.0052$). Thus, there is a significant association of RPN2 expression with the pathologic response to docetaxel. Although the data are not shown, RPN2 mRNA expression was significantly increased in cancerous tissues compared to that in normal tissues.

Furthermore, we also assessed validated sets of new samples from 26 subjects with breast tumors (12 responders and 14 nonresponders). The expression of RPN2 was higher in nonresponders than in responders (nonresponders, 0.240 ± 0.066, versus responders, 0.025 ± 0.194). Because of the small sample size in the validation set, we have not obtained conclusive results at this time. We are currently seeking larger samples that will be tested in the near future. However, when we combined studies with subjects in the learning and validation sets, RPN2 expression was significantly higher in nonresponders (34 subjects) than in responders (36 subjects) (nonresponders, 0.306 ± 0.046, versus responders, 0.080 ± 0.075; $P = 0.0219$).

Downregulation of RPN2 in orthotopic breast tumors

To extend our *in vitro* findings and to determine whether RPN2 could be an effective therapeutic target for docetaxel-resistant breast cancer, we examined the effect of RPN2 siRNA on an animal model of breast tumors by orthotopically implanting MCF7-ADR cells into mice and using an atelocollagen-mediated *in vivo* siRNA delivery[21,22]. We injected the RPN2 siRNA or nontargeting control siRNA (1 nmol per tumor) with 0.5% atelocollagen in a 200 µl volume into tumors that had reached 4–5 mm in diameter 7 d after inoculation of MCF7-ADR cells. At the time of siRNA administration, docetaxel was intraperitoneally (i.p.) injected into the mice. Subsequent tumor development was monitored by measuring the tumor size for a week. Mice that had been administered the RPN2 siRNA–atelocollagen complex and docetaxel (20 mg kg^{-1} i.p.) showed a significant decrease in tumor size (mean ± s.d.; day 0, 52 ± 8 mm^3; day 7, 21 ± 8 mm^3) relative to mice that had been administered the control nontargeting siRNA–atelocollagen (day 0, 37 ± 7 mm^3; day 7, 35 ± 12 mm^3; $P < 0.01$) (**Fig. 4a**). The tumor size was markedly reduced by administration of RPN2 siRNA with docetaxel at 7 d after treatment (**Fig. 4b**). In the absence of docetaxel, RPN2 siRNA treatment slightly reduced MCF7-ADR tumor size relative to controls; however, there were no statistically significant differences (**Supplementary Fig. 3a** online). We also observed that docetaxel alone had no significant effect on tumor growth (**Supplementary Fig. 3a**). Furthermore, no significant differences were observed in tumor growth between mice treated with control nontargeting siRNA and untreated mice in the presence or in the absence of docetaxel (data not shown). Thus, RPN2 siRNA is useful for reducing the size of orthotopic MCF7-ADR breast tumors in the presence of docetaxel. Additionally, to evaluate the effect of sustained treatment with siRNA, we treated mice with tumors twice by injection of siRNA-atelocollagen complex. RPN2 siRNA or nontargeting control siRNA (1 nmol per tumor) were injected into the tumors (diameter, 4 mm) at days 0

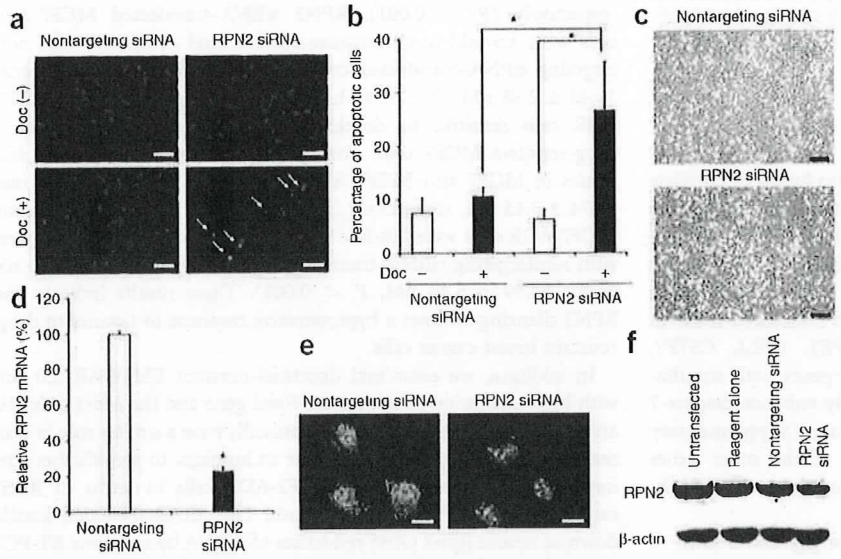

Figure 2 Apoptosis of MCF7-ADR cells transduced with RPN2 siRNA. (**a**) Hoechst staining of cells in the presence or absence of docetaxel (Doc, 1 nM) 72 h after the transfection of RPN2 siRNA. Scale bar, 50 µm. The arrows indicate cells with nuclear condensation and fragmentation. (**b**) Numbers of apoptotic cells from **a**. The data show the percentage of apoptotic cells in the presence or absence of docetaxel (1 nM) 72 h after the transfection of RPN2 siRNA. As a control, nontargeting control siRNA was used ($n = 4$ per group, $^*P < 0.02$). (**c**) Phase-contrast micrograph of MCF7-ADR cells 72 h after treatment with RPN2 siRNAs or control nontargeting siRNAs in the presence of docetaxel. Scale bar, 200 µm. (**d**) Knockdown of RPN2 mRNA by RPN2 siRNA in a cell transfection array, as monitored by cell-direct real-time RT-PCR analysis. As a control, nontargeting siRNA was used ($n = 4$ per group, $^*P < 0.001$). (**e**) Immunofluorescence staining of the RPN2 protein in MCF7-ADR cells 72 h after treatment with RPN2 siRNAs or control nontargeting siRNAs. Scale bar, 5 µm. (**f**) Western blot analysis of RPN2 protein in MCF7-ADR cells treated with RPN2 siRNAs or control nontargeting siRNAs 72 h after the liposome-mediated transfection. Values are means ± s.d.

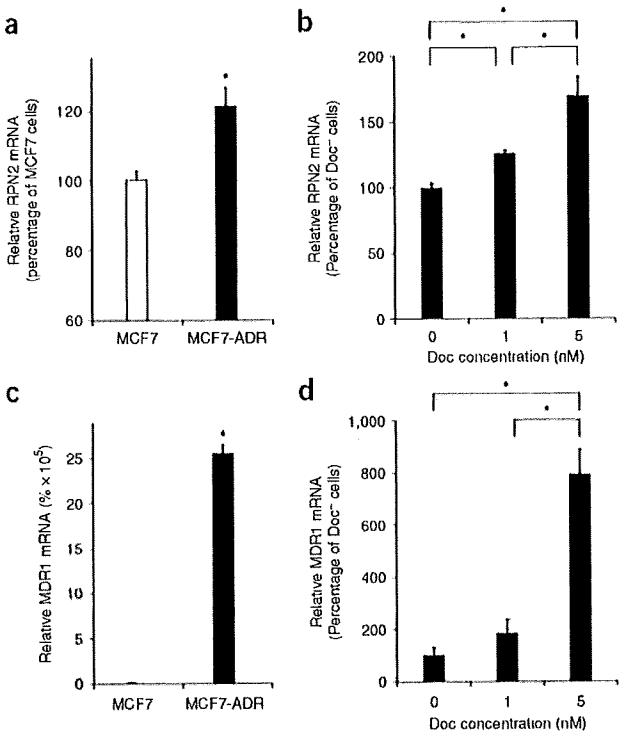

Figure 3 Induction of RPN2 and MDR1 expression by docetaxel treatment. RPN2 mRNA and MDR1 mRNA expression were analyzed by real-time RT-PCR. (**a**) RPN2 expression in drug-resistant MCF7-ADR cells and parental drug-sensitive MCF7 cells ($n = 3$ per group, $^*P < 0.01$). (**b**) Expression of RPN2 induced by docetaxel treatment in parental MCF7 cells. The data shown are from 48 h after the treatment ($n = 3$ per group, $^*P < 0.01$). (**c**) MDR1 expression in drug-resistant MCF7-ADR cells and parental drug-sensitive MCF7 cells ($n = 3$ per group, $^*P < 0.001$). The numbers on the *y* axis represent percentage ($\times 10^5$) of MCF7 cells. (**d**) Expression of MDR1 induced by docetaxel treatment in parental MCF7 cells. The data shown are from 48 h after the treatment ($n = 3$ per group, $^*P < 0.01$). Values are means ± s.d.

and 10. Simultaneously, docetaxel (20 mg kg^{-1} i.p.) was injected into the mice. We observed the mice for 20 d. Mice that had been given RPN2 siRNA and docetaxel showed significantly suppressed tumor growth relative to the mice that were administered control nontargeting siRNA at day 20 after the treatment ($P < 0.05$, **Supplementary Fig. 3b,c**). Mice showed no toxic effect during the observation period.

Furthermore, we examined the effect of RPN2 siRNA on a second animal model of breast tumors by orthotopically implanting MDA-MB-231/MDR1 cells. First, we established an MDA-MB-231/MDR1 cell line, which expresses the *MDR1* gene inducing docetaxel resistance. In this study, MDR1 expression is a key factor, because we are proposing that the coordinate expressions of RPN2 and P-glycoprotein may participate in the mechanism of docetaxel resistance. We injected the RPN2 siRNA or nontargeting control siRNA (2 nmol per tumor) with 0.5% atelocollagen in a 200 µl volume into tumors that were 5–6 mm in diameter 8 d after inoculation of MDA-MB-231/MDR1 cells. At the same time of siRNA administration, we injected docetaxel i.p. into the mice. Because docetaxel at a dose of 20 mg kg^{-1} in mice slightly suppressed MDA-MB-231/MDR1 tumor growth, we reduced the dose of docetaxel to 7 mg kg^{-1}, corresponding to the IC_{50} value of docetaxel in MDA-MB-231/MDR1 cells, which was 35% of that of MCF7-ADR cells. At a dose of 7 mg kg^{-1} docetaxel, mice treated with docetaxel alone showed no significant change in tumor growth. Subsequent tumor development was monitored by measuring the tumor size for a week. Mice that had been administered the RPN2 siRNA–atelocollagen complex and docetaxel (7 mg kg^{-1} i.p.) showed a significant inhibition of tumor growth (day 0, 61 ± 21 mm^3; day 7, 97 ± 24 mm^3) relative to mice that had been administered the control nontargeting siRNA–atelocollagen complex (day 0, 68 ± 9 mm^3; day 7, 154 ± 23 mm^3) (**Fig. 4c,d**). The value was statistically significant, with $P < 0.002$. Tumors treated with RPN2 siRNA in the absence of docetaxel showed no significant inhibition relative to control tumors that had been given nontargeting siRNA or docetaxel alone (data not shown). These results show that the growth of docetaxel-resistant MDA-MB-231/MDR1 tumors was suppressed by administration of RPN2 siRNA and docetaxel. Thus, RPN2 silencing is effective for the suppression of tumor growth in two models for docetaxel-resistant breast cancer in the presence of docetaxel.

RPN2 siRNA delivery augments docetaxel-induced apoptosis

MCF7-ADR tumors treated with RPN2 siRNA were investigated for apoptotic activity after docetaxel treatment for 3 d. TUNEL staining of tumor tissue treated with RPN2 siRNA revealed a significant number of apoptotic cells relative to the number in nontargeting control siRNA–treated tumors ($P < 0.01$, **Fig. 4e,f**). In contrast, RPN2 siRNA–transduced tumors in the absence of docetaxel showed no marked apoptotic cell death (**Fig. 4e,f**). We have also previously shown that atelocollagen alone does not induce any cytotoxic or inflammatory effect when it is injected into mice[23,24]. In a subsequent experiment, the mRNA levels of RPN2 in treated tumors were measured. RPN2 expression was significantly reduced in mouse tumors after combined treatment with RPN2 siRNA and docetaxel ($P < 0.05$, **Fig. 4g**). Furthermore, the RPN2 protein abundance in treated tumors was markedly downregulated by RPN2 siRNA (**Fig. 4h**). Thus, these results altogether indicate that RPN2 siRNA induces tumor inhibition via augmentation of docetaxel-induced apoptotic cell death *in vivo*.

To examine docetaxel retention in the tumors in the *in vivo* experiment, we performed drug disposition analysis. Eleven hours after docetaxel administration, we dissected the tumors and determined the amount of docetaxel incorporated into the tumors by HPLC with ultraviolet detection at 225 nm after solid-liquid extraction. We detected docetaxel in tumors that had received RPN2 siRNA ($n = 4$) at a range of 667 to 1400 ng per wet gram of tissue (**Fig. 4i**). In contrast, the tumors that received control siRNA ($n = 4$) showed a very low amount of docetaxel (~10 ng per wet gram of tissue). Thus, the results clearly indicate that abrogation of RPN2 expression in drug-resistant tumors results in docetaxel accumulation in those tumors.

RPN2 siRNA reduces *N*-linked glycosylation of MDR1

The mammalian *RPN2* gene encodes a type I integral membrane protein found only in the rough endoplasmic reticulum[25,26]. The RPN2 protein is part of an *N*-oligosaccharyl transferase complex that links high mannose oligosaccharides to asparagine residues found in the N-X-S/T consensus motif of nascent polypeptide chains[27]. The expression of the multidrug transporter P-glycoprotein, encoded by *MDR1*, is one of the causes of clinical drug resistance to taxanes. Real-time RT-PCR analysis showed that MCF7-ADR cells expressed abundant MDR1 mRNA, whereas parental cells did not (**Fig. 3c**). In addition, the MDR1 mRNA amount was not significantly decreased